ARL 59

STUDIES OF THE PARTICLE-IMPACT PROCESS FOR APPLYING CERAMIC AND CERMET COATINGS

D. G. MOORE
A. G. EUBANKS
H. R. THORNTON
W. D. HAYES, JR.
A. W. CRIGLER

NATIONAL BUREAU OF STANDARDS

AUGUST 1961

AERONAUTICAL RESEARCH LABORATORY
OFFICE OF AEROSPACE RESEARCH
UNITED STATES AIR FORCE

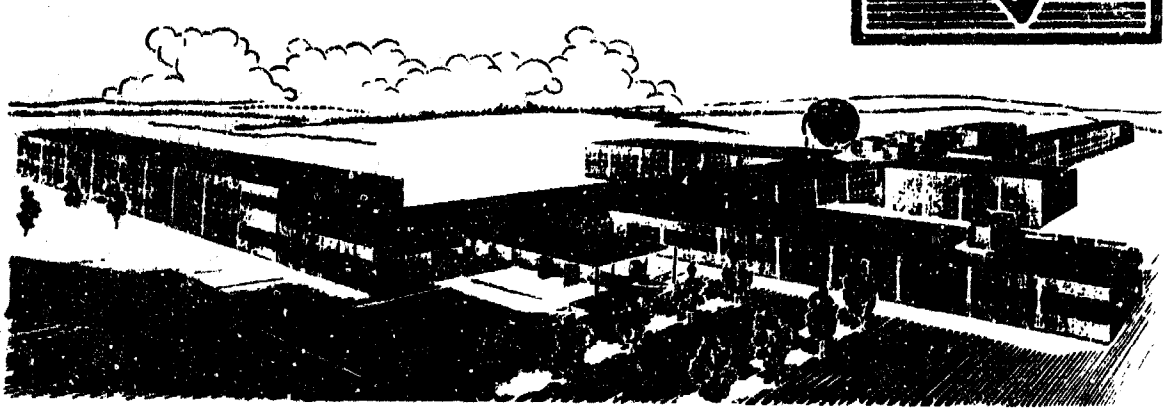

NOTICES

When Government drawings, specifications, or other data are used for any purpose other than in connection with a definitely related Government procurement operation, the United States Government thereby incurs no responsibility nor any obligation whatsoever; and the fact that the Government may have formulated, furnished, or in any way supplied the said drawings, specifications, or other data, is not to be regarded by implication or otherwise as in any manner licensing the holder or any other person or corporation, or conveying any rights or permission to manufacture, use, or sell any patented invention that may in any way be related thereto.

Qualified requesters may obtain copies of this report from the Armed Services Technical Information Agency, (ASTIA), Arlington Hall Station, Arlington 12, Virginia.

This report has been released to the Office of Technical Services, U. S. Department of Commerce, Washington 25, D. C. for sale to the general public.

Copies of ARL Technical Reports and Technical Notes should not be returned to Aeronautical Research Laboratory unless return is required by security considerations, contractual obligations, or notices on a specific document.

AF-WP-L-FEB 61 500

ARL 59

STUDIES OF THE PARTICLE-IMPACT PROCESS FOR APPLYING CERAMIC AND CERMET COATINGS

D. G. MOORE
A. G. EUBANKS
H. R. THORNTON
W. D. HAYES, JR.
A. W. CRIGLER

NATIONAL BUREAU OF STANDARDS

AUGUST 1961

CONTRACT No. AF 33(616)-58-19
PROJECT 8(68-7022)
TASK 70864

AERONAUTICAL RESEARCH LABORATORY
OFFICE OF AEROSPACE RESEARCH
UNITED STATES AIR FORCE
WRIGHT-PATTERSON AIR FORCE BASE, OHIO

McGregor & Werner, Inc., Dayton, O.
300 - November 1961 - 7-216 & 217

FOREWORD

This report was prepared by the Enameled Metals Section, Mineral Products Division, National Bureau of Standards under USAF Contract No. AF (33-616)58-19. The contract was initiated under Project No. 8(98-7022), "Surface and Interface Phenomena of Matter", Task 70664, "Compacting and Sintering of Powders; Basic Mechanisms and Influence of Surface Conditions and Environment." The work was administered by the Aeronautical Research Laboratories with Murray A. Schwartz acting as Project Engineer from July 1, 1958 to Feb. 1, 1959 and Capt. Harry F. Rizzo from Feb. 1, 1959 to July 1, 1960.

The present report is a final Summary Report of the investigation.

ABSTRACT

A basic study was made of the particle-impact process for applying coatings of aluminum oxide. One rod-type and two powder-type flame-spraying guns were used in the work.

The coatings were found to consist primarily of the softer eta phase rather than the harder and more stable alpha form of alumina. It was established that the eta phase forms because of the high quenching rates. Calculated quenching rates were of the order of 800,000°C/sec. on a stainless steel substrate, and 34,000°C/sec. on glass.

Size and velocity measurements were made for particles from both gun types. High-speed motion pictures showed that the powder guns sprayed particles continuously; the rod gun in bursts.

Most of the particles from both gun types were found to be molten at normal spraying distances. Severe deformation and radial flow occurred when they struck a smooth surface. For the relatively low velocity powder-gun particles, the flow on a glass substrate sometimes resembled that of a water drop striking a smooth plate. At high velocities (rod gun spraying) the molten particles appeared to be atomized into very small droplets when they struck a polished metal. On a roughened surface, however, there was little of this effect.

The coating layer on an iron substrate was shown to be under compression at room temperature. This compression attenuated on heating and changed to tension at higher temperature. A residual stress gradient was found to be present in the coating layer after it was removed from the iron.

A chemical bond sufficient to withstand interfacial stresses without spontaneous failure was developed between the coating and smooth glass substrates, but never between the coating and smooth metal. It was shown that the apparent bond strength between the coating and iron increased exponentially with increasing roughness of an iron surface, rather than linearly, which would be expected if the bond was chemical. Strong bonds were obtained on smooth iron specimens that had been oxidized in steam. However, the outer surface of oxide was found to be rough. When this outer surface was polished prior to flame spraying the alumina layer no longer adhered.

TABLE OF CONTENTS

TABLE OF CONTENTS (cont.)

LIST OF ILLUSTRATIONS

LIST OF ILLUSTRATIONS (cont.)

LIST OF TABLES

I. INTRODUCTION

In particle-impact processes such as flame-spraying (1) (2),* flame-plating (3), and plasma-jet spraying (4) a coating is formed by projecting small high-speed particles against a metal surface. When such coatings are formed of suitable ceramics and cermets they are hard and refractory, and because of these properties, they have numerous potential uses for missiles, rockets, and space vehicles.

The layered structure of most particle-impact coatings suggests that the particles are molten before they strike a surface and after striking they flatten and freeze. This implied mechanism may be correct. However, a more detailed understanding of this and other facets of the process would be desirable in order to devise coatings with improved properties. In particular, more needs to be known about (a) the size and shape of the particles in spray, (b) their cooling rates during travel and after striking a given substrate, (c) their flow behavior on impact, (d) the mechanisms responsible for bonding of the coating to the substrate, and (e) the origin and magnitude of stresses in the system.

A basic study aimed at obtaining information of this type was carried forward from July 1, 1958 to July 1, 1960 under USAF Contract No. 33 (616) 58-19. The present report constitutes a final summary report of the investigation. In all of the experimental phases of the work, aluminum oxide was the sprayed material and oxy-acetylene flame-spraying guns were used for melting and propelling the particles.

Manuscript released by authors, April 1961, for publication as an ARDC Technical Report.

*Numbers in parentheses refer to the list of references at the end of this report.

II. PREVIOUS WORK

Although the particle-impact process for applying metallic coatings has been known since 1910 (5), the basic principles that govern the forming of coatings by this process are not well understood. One of the first attempts to obtain such an understanding was made in Germany by Matting and Becker (6). These authors were the first to use high-speed photography to study (a) the melting of the metal at the tip of the wire and the subsequent atomization of the molten material, (b) the velocity of the particles in the spray beam, and (c) the flow behavior of the oxide that formed both on the metal wire and on the atomized metal particles. The belief of these authors at the completion of the investigation was that an oxide film surrounds each metal particle (steel and copper alloys were used) during flight and that this film is torn away at the instant of impact. Thus, clean metal contacts clean metal and good local welding results. In addition, they believed that the particles were not molten at the time of impact, but rather that particle flattening occurred by plastic deformation of the metal.

Ault (1) published the first comprehensive report on the flame-spraying of ceramic oxides with a rod-type gun. This report, however, was concerned almost entirely with the properties of the coatings and no attempt was made to investigate the basic mechanisms of the process.

Galli, et al, (7) recognized the need for a more thorough understanding of the flame-spray process while attempting to develop composite coatings for rocket nozzles. To fill this need, the velocities of alumina particles from a powder gun were measured. Heat transfer calculations were then applied and these computations showed that particles of the size used in the gun (30μ avg diam) should be completely molten by the time they reached the substrate. However, other evidence suggested that only surface melting had occurred. The authors point out that the lowering of the melting point that results from small particle radius may be important in the flame spray operation. Their calculations showed that the melting point of alumina could be lowered by as much as 135°C when the radius was reduced to 0.1μ. The authors state that while very few particles with this radius are in the spray, the effect is nevertheless active on the rough, irregular corners of the alumina powder particles that are introduced into the gun. Because these corners are rounded by localized melting during spraying, it is possible to have a rounded particle without the surface ever reaching the reported melting temperature of the material. The authors state in their conclusions that their experiments with alumina "indicate almost beyond doubt that the particles are partially solid when they strike the test part."

A more recent report on the flame spraying of ceramic oxides was published by Meyer (8). The sprayed material was aluminum oxide. A powder gun was used. The gases were propane and oxygen. The investigation was concerned with (a) the mechanism of coating formation (b) coating properties, and (c) the bond mechanism. One of the more interesting observations in this study was that coatings with the greatest hardness and lowest porosity were formed when the impinging particles were molten at the moment of impact; also, that the optimum hardness and porosity were achieved when spraying the larger-sized particles.

III. FLAME SPRAY GUNS

Three commercial oxy-acetylene flame-spray guns were used in the investigation. Gun A was a rod type similar to that described by Ault (1) while guns B and C were powder.

In powder gun B, the dry powder is fed into the gun through a rubber tubing that is connected to a storage hopper placed several feet away. During operation the powder flows, with the aid of a vibrator, into a small tube at the bottom of the hopper where it is picked up by an air stream and carried into the gun nozzle. The small amount of air needed for transporting the powder through the rubber tubing is aspirated from the gun nozzle. Powder feed is controlled by an adjusting screw at the bottom of the hopper.

The hopper of powder gun C is attached above the gun and the feed is by gravity aided by a vibrator. Powder feed is controlled to an adjusting screw placed at the base of the hopper. This gun (gun C) was obtained late in the investigation; hence, much of the data for powder gun spraying are reported for gun B.

The two powder guns operate with oxygen and acetylene gas only. However, in the rod gun air at 80 psi is added at the nozzle to increase particle acceleration.

Unless otherwise stated, all three guns were operated at the gas pressures and feed rates recommended by the manufacturers (see Table 1). The alumina powders and rods were those supplied by the manufacturers. The alumina used for the rods was of commercial purity. The powder for powder gun B contained an estimated 3 percent by weight admixture of rutile (TiO_2). The manufacturer of gun C supplied two powders. One powder (101) contained 2.5 percent by weight titanium oxide (5); the other(powder 105) consisted of commercially pure alumina with no admixtures.

TABLE 1.

OPERATING CONDITIONS OF FLAME-SPRAY GUNS

	Rod Gun A	Powder Gun B	Powder Gun C
Type of feed	1/8" rod	powder	powder
Feed rate (g/min)	3.4[a/]	15	15
Oxygen pressure (psig)	25	25	25
Acetylene pressure (psig)	15	15	15
Air pressure (psig)	80	-	-
Oxygen flow rate (Cu ft/hr)	59	59	59
Acetylene flow rate (Cu ft/hr)	34	34	34
Air flow rate (Cu ft/hr)	1545	-	-

a/ Equivalent to 6½ in/min

High speed motion pictures (16mm, 8000 frames/sec) showed that while the two powder guns sprayed particles continuously the rod gun sprayed particles in a series of short bursts. As indicated in Figure 1, the percentage of time that the rod gun was spraying particles was dependent on the feed rate. A rough extrapolation of the data suggests that a feed rate of about 12 in/min would be required to obtain a continuous spray from the 1/8" diam.rod. With the gun that was used, however, feed rates above 10 in/min produced a spray that contained a few large unmelted fragments.

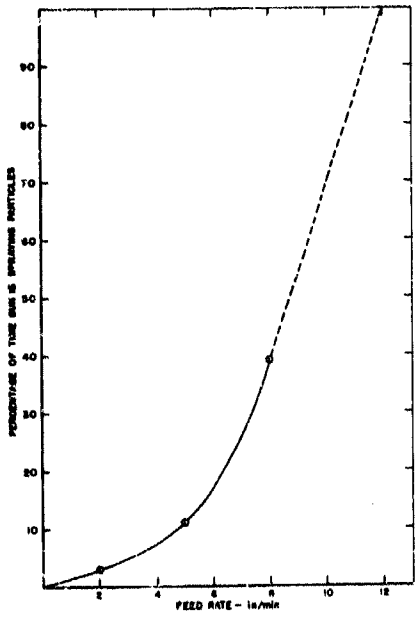

Figure 1. Percentage of time particles were in spray of rod gun A when gun was operated with 1/8" diam.rods of alumina.

IV. STRUCTURE AND HARDNESS OF ALUMINA COATINGS

The structure and hardness of both flame-plated* and flame-sprayed (rod gun) coatings of alumina were investigated in the initial phases of the study. Small ½ x 3 x 0.045 in. specimens of copper, ingot iron, 18-8 stainless steel and 17-7PH (both hard and soft) were grit blasted after which they were coated with alumina. The powder gun coatings were applied in this laboratory while the rod-gun and flame-plated coatings were applied by experienced outside organizations. In each case, the coating was applied at 0.005 ± 0.001 in.

4.1 Crystal Structure

X-ray diffraction patterns were made of the surfaces of both flame-sprayed (rod gun) and flame-plated specimens. The equipment consisted of a Norelco diffractometer with a copper target.

*In the flame plating process, oxygen and acetylene are metered into a shock tube along with the powder that forms the coating and the mixture detonated. The process in current use, which is fully mechanized, provides for four detonations per sec.

The spacings and relative intensities of the diffraction peaks from the two coatings are listed in Table 2 along with similar data for eta, gamma, and alpha alumina. The differences in spacings and intensities of the peaks in the two coatings are minor and they can be considered as consisting of the same phase. Identification of this phase could not be made with certainty from available standard patterns, but the observed pattern comes closest to matching that of eta alumina. According to Russell, et al, (9), it is difficult to distinguish between the eta and gamma forms, and they state that the characterization of gamma is usually based on the 1.98 - 195Å doublet and equal intensities of the 2.41 and 2.28Å peaks, rather than on the absence of the 4.6Å peak. Using this criterion, it is obvious from Table 2 that eta is a more likely phase in the coating than is gamma. Ault (1) reported gamma to be present in a rod-gun coating while Meyer (8) reported delta alumina in a coating applied with a powder-gun.

The presence of lines at 2.50 and 1.62Å suggests that a small amount of alpha phase is present in both coatings. Later examination of other alumina coatings applied by both plasma-jet spraying (supplied by an outside laboratory) and a powder-gun (gun B) showed strong peaks at these two spacings. The second phase in both of these coatings was identified as eta alumina.

TABLE 2.

X-RAY DIFFRACTION DATA FOR TWO ALUMINA COATINGS AND FOR THREE FORMS OF ALUMINUM OXIDE

Flame-sprayed Alumina[a/]		Flame-plated Alumina		Eta[b/] Alumina		Gamma[b/] Alumina		Alpha[b/] Alumina	
d	I	d	I	d	I	d	I	d	I
4.62	7	4.72	7	4.60	40				
2.81	15	2.81	8					3.48	80
2.74	16	2.78	9			2.70	20		
2.62	9								
2.50	9	2.53	211					2.55	90
2.40	33	2.40	27	2.40	60	2.41	60	2.38	70
2.29	16	2.28	22	2.27	30	2.28	60		
						2.18	20		
						2.09	10	2.08	100
1.987	100	1.980	98	1.97	80	1.98	100		
						1.95	60	1.74	80
						1.54	20		
1.622	3	1.612	5					1.60	100
1.525	15	1.519	12	1.52	20			1.51	40
1.402	79	1.398	100	1.40	100	1.39	100	1.40	70
								1.369	100

d is line spacing in Å; I is relative intensity of line.
a/ Applied with rod-type gun
b/ Values taken from reference 9.

Additional information on crystal structure is included in Section VI.

4.2 Microstructure

Metallographic sections were prepared from the flame-plate and rod-gun coatings of each of the metals and of the two coatings and coating-metal interfaces. The rod-gun coating (Fig. 2B) shows a well developed structure similar to that observed by Ault (1). Bonding between the flattened particles is better than might be implied from the micrograph. The boundaries are almost undetectable in vertical illumination and additional illumination at a low angle is necessary to achieve the definition illustrated in the figure. It is probable that the grain-boundary material is removed faster during polishing than the grains themselves, thus causing the grains to stand out in slight relief when viewed with low-angle illumination. That the grains are fairly well bonded is indicated by the 1000 psi modulus of rupture value obtained by Ault (1) for alumina specimens prepared by rod-gun spraying, and tested with the stress applied normal to the coating surface.

Individual grains are not detectable on the flame-plated specimen (Fig. 2C). There is, however, a slight evidence of laminations. These laminations probably formed, as in the case of the rod gun, by the deposition of new particles on the partially-cooled coating layer. The smaller particle size and appreciably higher particle velocity of the flame-plate detonation process (3) is undoubtedly responsible for the observed absence of a pronounced laminated structure.

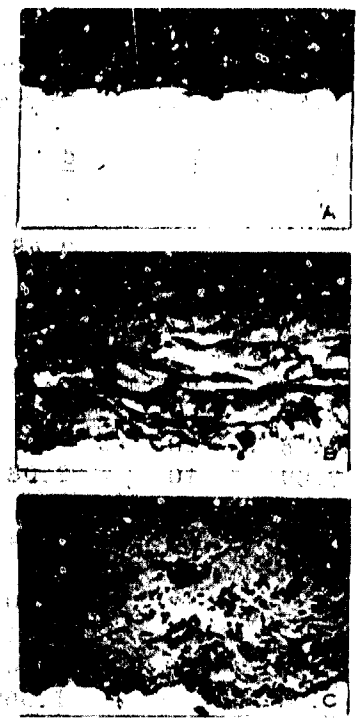

Figure 2. Microstructures of A) uncoated but grit-blasted stainless steel, and of B) rod gun alumina coating, and C) flame-plated alumina both on grit-blasted stainless steel. A) was taken with vertical illumination; B) and C) with vertical plus oblique illumination. Unetched.

Pores were present in both types of coatings but the pores were both larger and more numerous in the rod-gun coating than in the flame-plated.

The micrographs of Figure 2 were taken of unetched surfaces. Later in the investigation an etching procedure was found that helped to bring out structure. The etch consisted of immersing polished sections in 85% orthophosphoric acid at 160°C (320°F) for periods ranging from 30 sec. to 2 min.

Figure 3 is representative of the structures observed after this etching treatment. Laminations and pores are more clearly defined than in Figure 2, especially for the flame-plated coating. Grain boundaries in the sections parallel to the interface are clearly defined in the powder-gun and rod-gun coatings but not in the flame-plated. The powder gun coating was applied in the Bureau laboratory with powder gun B.

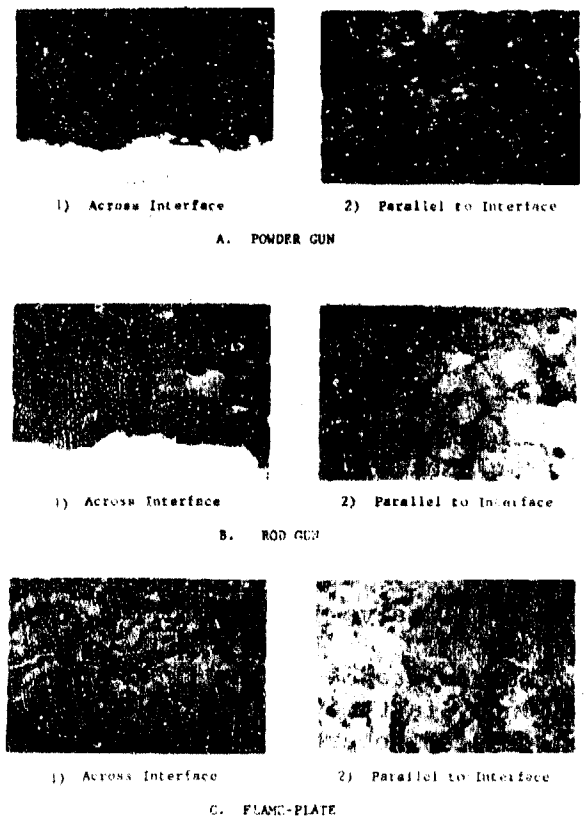

Figure 3. Micrographs of flame-sprayed alumina surfaces etched in 85% orthophosphoric at 320°F. Etching time for A and B was 30 sec., for C, 2 min. Micrographs labeled "across interface" were taken of cross-sections through the coating-metal interface while those labelled "parallel to interface" show a plane through the interior of the coating normal to the coating surface.

4.3 Microhardness

Microhardness measurements were made on polished surfaces of five particle-impact coatings and also on polished surfaces of a sintered alumina ceramic and a sapphire crystal. In the case of the coatings, care was taken to select areas that were free of pores.

Table 3 gives the results. The comparatively low hardness numbers for the coatings are believed to reflect the presence of the eta alumina. Both the sapphire and the alumina body consist of the harder alpha or corundum phase. The lower microhardness of the sintered alumina body over that of the sapphire is undoubtedly caused by the weakening effect of the grain boundaries present in the sintered structure.

TABLE 3.

VICKERS AND KNOOP HARDNESS NUMBERS FOR FIVE PARTICLE-IMPACT COATINGS FOR A SINTERED ALUMINA BODY, AND FOR A SINGLE CRYSTAL OF ALUMINA

Material	Vickers Hardness Number[a] (150g load)	Knoop Hardness Number[b] (700g load)
Flame-sprayed alumina		
Rod gun A	908	692
Powder gun B	[c]	731
Powder gun C (101 powder)	[c]	756
Powder gun C (105 powder)	[c]	725
Flame-plated alumina	935	767
Sintered alumina body	1236	1294
Single crystal alumina (sapphire)[d]	2103	1762

a/ Avg. of three measurements on polished surfaces.
b/ Avg. of seven measurements on polished surfaces.
c/ Not determined.
d/ Measured on a crystal surface that deviated about 4° from (303) plane; c axis was inclined at approx. 45° to specimen surface.

4.4 Abrasive jet hardness

The resistance of the two types of coating (rod gun and powder gun) to abrasion by fast-moving particles was determined with an instrument described previously by Roberts (10). A brief description of the equipment and its operation follows:

Alumina powder with a mean particle diameter of 27μ is carried by carbon dioxide gas through a nozzle with a diameter of 0.02 in. The alumina powder is fed into the gas stream at a rate of 6 grams per min. The specimen is positioned normal to the nozzle axis at a distance of 0.4 in. During operation the carbon dioxide pressure is maintained constant at 50 psi. The resistance of a coating is determined by measuring the time for the abrasive jet to penetrate the layer and reach the metal substrate. The abrasion rate is the coating thickness in mils divided by the penetration time in seconds.

Table 4 gives the results. The particle-impact coatings are listed in order of decreasing abrasion resistance. The flame plate has the highest resistance. This is undoubtedly due to the small number of pores and to the strong bonding of particles in the flame-plate structure (see Fig. 2 and 3). The two powder-gun coatings that contained titanium oxide showed a relatively high resistance to the test conditions. The results with powder gun C are of particular interest. Powder 101, which contains 2.5 weight percent titania, gave a coating with an abrasion rate of 0.93 mils/sec. The coating formed from 105 powder, which is commercially pure alumina, showed a resistance to the abrasive jet conditions that was lower than the 101 coating by a factor of 4. This implies that when titania is present the structure is strengthened. The rod gun coating, which is formed also of commercially pure alumina, showed an abrasion resistance comparable to the powder gun coating applied with the 105 powder.

The last three coatings listed in Table 4, which are organic, are included for comparison. The neoprene base coating has an especially high resistance, probably because of its resilience. Such a coating would of course be unsuitable for use at elevated temperatures.

TABLE 4.

ABRASION RATES AT ROOM TEMPERATURE

Material	Abrasion Rate[a/] mils/sec.
Flame-plated alumina coating	0.86
101 alumina coating-powder gun C[b/]	0.93
Alumina coating-powder gun B[b/]	1.47
105 alumina coating-powder gun C	3.61
Alumina coating-rod gun A	3.86
Automative lacquer[c/]	2.50
Neoprene base coating[c/]	0.04
Vynl base coating[c/]	0.77

a/ Rate of coating removal by an abrasive jet. See Ref. 10 for testing procedure.
b/ Coating contains approximately 3% by weight of TiO_2.
c/ Data furnished by A. G. Roberts of the NBS Organic Building Materials Section.

V. SIZE AND VELOCITY OF PARTICLES

5.1 Particle size

The arithmetic average size of particle was obtained for particles collected from both the rod gun and powder gun B in normal operation. The particles were collected from the powder gun by spraying into water, but this method was found unsuited for the rod gun because of the high-velocity gas stream. Hence, the sample from the rod gun was collected by spraying onto ice cubes placed in a cylindrical container.

Examination of the rod-gun sample with a microscope showed that all the collected particles consisted of small spheres of varying diameter. The particles introduced into the powder gun were sharp edged. After spraying approximately 95% were spheres and the remainder showed either rounding of edges (partial melting) or sharp edged geometry (no melting). In almost all cases, the unmelted particles occurred in the larger size fraction.

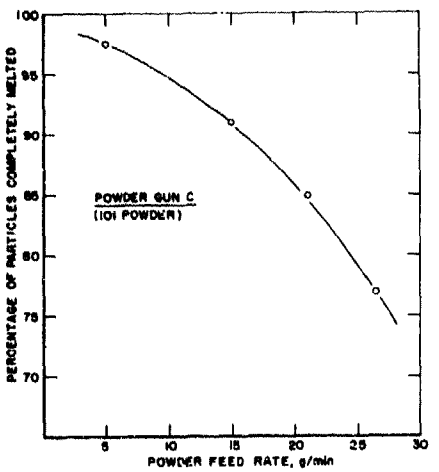

Figure 4. Effect of feed rate on particle melting for powder gun C.

Later work with powder gun "C" showed that the percentage of particles that are melted during spraying with a powder gun is dependent on feed rate. This is shown by the data plotted in Figure 4. The particles from which this analysis was made were collected in a water soluble gel* that had been spread on a 1/16 in. thick film over a glass microscope slide. The gun was passed quickly in front of the slide. The imbedded particles were then examined with a microscope.**

The following is a summary of measurements made with the microscope of the two samples that were collected by spraying into water (powder gun) and onto ice (rod gun):

	Particle Size (μ)[a/]		
Type of Gun	Max.	Min.	Avg.
Rod Gun[b/]	28.7	0.8	6.4
Powder gun B	48.2	0.8	13.4

a/ Arithmetic average based on number of particles

b/ Reed rate - 6½ in./min. (1/8 in. rod)

The average diameter of the irregular-shaped fused alumina particles introduced into powder gun B was 12.7μ as against 13.4μ for the particles collected after passing through the flame. This difference is probably caused by the failure of the water collection system to trap all of the finer particles. The similarity of the two averages shows that there is little, if any, agglomeration of particles during powder gun spraying, or, stated differently, each particle appears to maintain its identity during spraying.

*K-Y Water Soluble Sterile Lubricant. Johnson and Johnson Co., New Brunswick, N. J.

**This method of collection misses most of the very small particles which, because of their low momentum, are carried away by the gas stream as it becomes diverted from a straight-line flow by the flat surface of the slide.

5.2 Particle velocity and dwell times

The three methods that were used for measuring the velocity of particles in the spray have been described in an earlier report (11). The results of these measurements are plotted in Figure 5. The reader is referred to the earlier report for details of the measuring procedures.

The dwell time of a particle is its time of residence in the hot gases and in flame spraying this may be taken as the travel time from the nozzle to the substrate. Average dwell times of particles at different spraying distances were computed from the velocity curves for powder gun B and for the rod gun. The results were as follows:

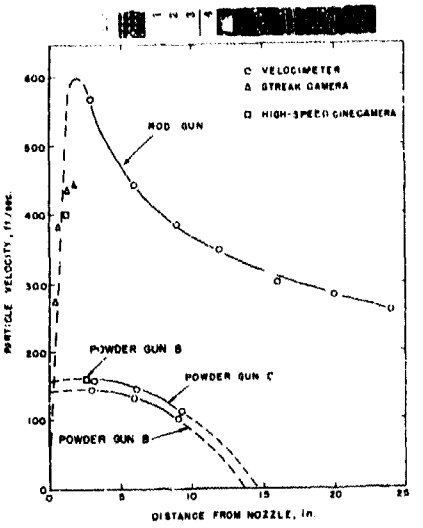

Figure 5. Measured particle velocities.

Spraying Distance (in.)	Time Required for Particles To Travel from Nozzle to Substrate	
	Powder Gun B (millisec.)	Rod Gun (millisec.)
3	1.8	0.5
5	3.0	0.8
8	4.8	1.2
12	7.2	1.9

These computations show that the particles from powder gun B travel 3 in. in about the same time (1.8 millisec.) that the particles from the rod gun travel 12 in. (1.9 millisec.).

An analysis of the possible penetration of the small high-velocity particles into metal substrates is given in Appendix I.

5.3 Effect of particle size on velocity

The velocity measurements that were made with a streak camera (11) suggested that particle size affected particle velocity. Because no method could be devised for determining accurately the diameter of the particle under observation in the streak camera measurements, it was impossible while working with a spray containing a wide range of particle sizes to establish experimentally the relation between the size of a particle in a spray and its velocity at impact.

In the case of the powder gun, however, the powder could be fractionated prior to spraying. The velocity of each size fraction could then be measured as it was sprayed under controlled conditions.

Powder gun C with type 105 powder was used for these experiments. The powder was first sprayed into water to spheroidize the particles. The resulting particles, after drying, were then separated into several size fractions with an air classifier.* Three of the fractions were recovered in amounts sufficient for the measurement of velocity with the rotating-disc velocimeter (11). These were designated as the 26μ, 17μ, and 11μ fractions. A size analysis of each is given in Table 5.

TABLE 5

SIZES OF PARTICLES IN FRACTIONS SEPARATED BY AIR CLASSIFIER

Nominal Size	Particle Sizes in Fraction		
	Size Range	No. of Particles	% of Particles
μ	μ		
11	6 - 8	0	0
	8 -10	15	3.7
	10 -12	155	58.9
	12 -14	93	35.4
	14 -16	0	0
17	10 -12	0	0
	12 -14	23	8.3
	14 -16	87	31.3
	16 -18	151	54.3
	18 -20	17	6.1
	20 -22	0	0
26	21 -23	0	0
	23 -25	19	9.4
	25 -27	158	78.6
	27 -29	23	11.4
	29 -31	1	0.6
	31 -33	0	0

The results of the velocity measurements for the three fractions are listed in Table 6. In each case, Powder gun C was used with normal operating pressures and feed rates; the rotating disc velocimeter measurements were made as previously described (11). The results are clear in showing that there is a dependence between size and velocity. In the first few inches of travel the small particles are accelerated to higher velocities than the larger particles. However, the small particles also decelerate faster, as they travel further downstream so that at a normal spraying distance (6 in.) all three particle fractions have velocities

*Haultain Infrasizer, Infrasizers Limited, 302 Mill Bldg., Univ. of Toronto, Toronto, Canada.

that differ by only 30 ft/sec. Such behavior might possibly be predicted from calculations based on gas velocities and gas densities, following for example, the procedures of Ingebo (12), but calculations of this type did not seem feasible for the powder gun operation because of the highly complex nature of the temperature, velocity, and composition gradients in the hot gases. The rod-gun spray is somewhat less complex because of the large volume of air added to the nozzle. Temperatures and velocities within this "flame" were measured and are listed in Table 7. A plot of the measured gas velocities at the flame axis against distance is plotted in Figure 6 together with the curve for the particle velocity as measured with the velocimeter (11). Calculation of particle velocoties from gas temperatures and gas velocities was not feasible in this case because of the wide range of particle diameters. Unfortunately no method could be devised that would permit the rod gun to spray a controlled size of particle.

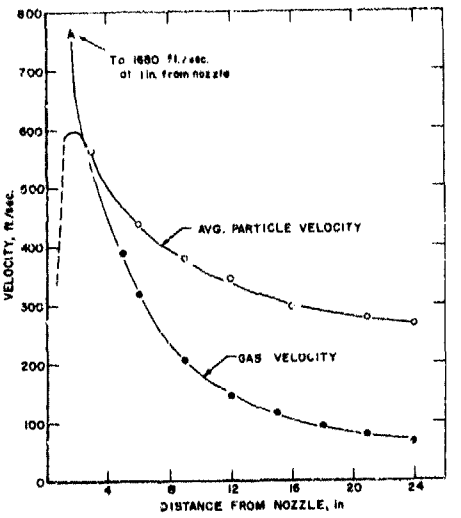

Figure 6. Comparison of gas stream and particle velocities for rod gun A at different distances from the nozzle.

TABLE 6.

VELOCITIES OF
DIFFERENT PARTICLE SIZE FRACTIONS

Nominal Particle Diam. μ	Measured Particle Velocity[a/] 3 in. from Nozzle ft/sec.	6 in. from Nozzle ft/sec.	9 in. from Nozzle ft/sec.
11	203	117	-
17	196	147	84
26	132	138	102

a/ Determined with rotating disc velocimeter (Ref. 11) for powder gun C spraying spheroidized particles of No. 105 alumina.

TABLE 7.

TEMPERATURES AND VELOCITIES MEASURED IN THE "FLAME" OF ROD GUN A OPERATING WITH NORMAL SETTINGS EXCEPT FOR NO ROD FEED

Distance from Nozzle	At Axis of Flame		5° from Flame Axis		10° from Flame Axis	
	Temp.[a]	Velocity[b]	Temp.[a]	Velocity[b]	Temp.[a]	Velocity[b]
in.	°C	ft/sec.	°C	ft/sec.	°C	ft/sec.
1	-	1680[c]	-	-	-	-
2	-	-	-	-	220	249
3	-	-	-	-	160	175
4	-	-	220	235	105	115
5	250	388	170	247	80	174
6	200	320	139	189	70	50
9	128	206	88	110	50	19
12	95	147	70	76	45	0
15	80	118	60	57	40	0
18	69	97	50	43	37	0
21	65	83	46	33	35	0
24	55	71	40	33	29	0

a/ Measured with an unshielded Pt; Pt-10% Rd thermocouple made of 0.010 in. diam. wires.

b/ Measured with a 0.050-in. diam. stainless steel pitot tube.

c/ From streak camera measurements (Ref. 11).

VI. STUDIES ON ETA ALUMINA FORMATION

The x-ray diffraction analysis described in Section 4.1 showed that eta alumina was the principle crystalline phase present in sprayed-alumina coatings. Eta is one of the metastable forms of alumina. As such, it has a lower thermal thermal expansion (1), density (1), and microhardness (see Sec. 4.3) than the more stable alpha form.

Ault (1) has shown that when an alumina coating formed by rod-gun spraying (and thus consisting of metastable alumina) is heated to elevated temperatures, it transforms to alpha alumina and that this transformation results in a linear shrinkage of approximately 3%. Ault found that while the transformation did not occur after three days at 1000°C, the coating converted completely in as short a time as 45 min. at 1460°C. Galli, et al, (7) tentatively ascribed the presence of the metastable phase in the coating to the rapid deceleration that occurs when the particles impinge on a cold substrate while Ault (1) inferred, as did Meyer (8), that the metastable phase was formed by the rapid quenching action.

6.1 Crystal phase of particles in collected samples

Particles from both the rod gun and powder gun B were collected by (a) spraying into a metal tube with an air filter at the far end, (b) spraying into a chamber filled with ice cubes, and (c) spraying into a container filled with water. The particles in the samples were then examined with a polarizing microscope. Alpha alumina is biaxial and appears bright when viewed under these conditions while all of the transitional phases are uniaxial or cubic and appear dark.

Examination of particles that were collected from the powder gun spraying showed alpha alumina to be the only phase present. Also, there was no particle flattening observed in the water or ice collections which suggests that the particles were decelerated before impact by a cushion of steam.

In the case of the rod gun collections, the smaller spheres were found to consist of a cubic phase while practically all of the larger spheres were alpha. The only large particles that were cubic were those few that had become flattened by contact with ice surfaces.

Thus, the observations with both guns are consistent with the viewpoint that alpha alumina crystallizes when the quenching rate of the particle is below a certain critical value, and that at higher quench rates, one of the transitional phases of alumina forms. When the rod gun was sprayed into the tube with a filter at one end, there was no impact until the particle had solidified. However, a quenching action would still be present because of the large volume of cold air added at the rod-gun nozzle. The small particles apparently cool rapidly because of this air blast and crystallize as a cubic phase of alumina.* The large particles cool more slowly and crystallize as alpha. In the case of the powder gun, no air is added to the spray. Hence, cooling takes place slowly and the particles solidify as alpha alumina. In fact, even when the particles from the powder gun are sprayed into water or onto ice, the quenching rates are apparently insufficient to produce one of the metastable forms of alumina.

6.2 Crystal phases in deposits flame sprayed on heated platinum.

If the viewpoint that the formation of eta alumina is caused by a fast quenching rate is correct, then it should be possible to form alpha alumina in a coating layer by reducing to a sufficiently low level the rate at which the particles cool when they strike a substrate. One simple way to reduce the quenching rate is to heat the substrate prior to spraying. Because the quenching rate should decrease with increased substrate heating, it should be possible by this approach to arrive at some critical substrate temperature above which the layer would consist entirely of alpha and below which only eta would form.

To determine if such an effect could be observed, powder gun B was used to spray platinum strips, 0.007 in. thick, that were heated by internal resistance. The temperature was controlled manually by adjustment of power input. Temperatures were measured by a high-speed recorder that was activated by a 36 gage Pt, Pt-Rh thermocouple, spot welded to the back of the specimen as separate wires.

*X-ray diffraction showed that the cubic phase was not identical with that found in the coating; the spacings suggested gamma rather than eta.

For each substrate temperature, the specimen was passed in front of the spray gun at a constant rate of 2.73 in./min. This gave a thin deposit that did not completely cover the platinum surface. After cooling this deposit was scraped from the surface and examined.

X-ray analyses showed the presence of both alpha and eta alumina in each of the deposits, but technical difficulties prevented quantitative measurement of the relative amounts. When the samples were examined under polarized light, however, estimates of the relative amounts of each phase could be made from the number of bright-appearing particles. This examination showed that the amount of alpha in the deposit increased as the temperature of the substrate increased. (see Figure 7).

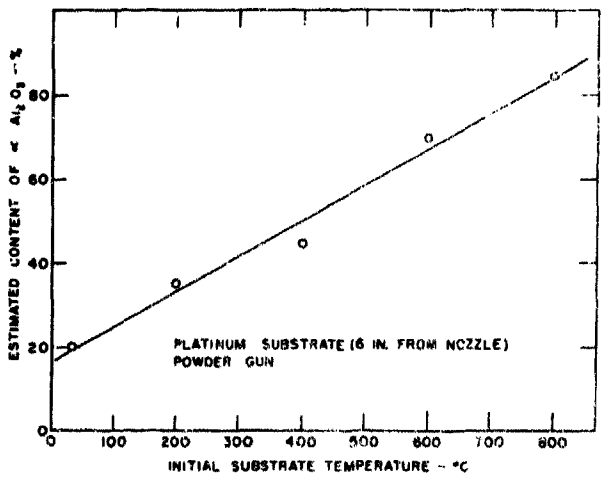

Figure 7. Effect of initial substrate temperature on alpha alumina content of a thin coating layer applied with powder gun B.

The highest substrate temperature used in the experiment was 800°C* which, according to the work of Ault (1), is too low for the deposit to transform to alpha alumina by a thermal inversion. Hence, the only plausible explanation for the increase in the alpha content with substrate temperature is that the particles striking the hotter substrates are cooled at a slower rate. The cooling rates vary with the size, velocity and temperature of the particles; therefore, a wide range of quenching rates at any one substrate temperature would be expected. This probably explains why there was no transition temperature above which only alpha was observed and below which only eta was present.

6.3 Discussion of theories to explain the formation of metastable alumina.

The experiments described in Sections 6.1 and 6.2 show that fast quenching rates prevent the formation of the stable alpha or corundum form of alumina. Instead, the particles crystallize as one of the transition phases. Such phases form during the calcination of certain aluminum compounds and, also, during the oxidation of aluminum. These intermediate phases, of which some eight or nine have been indexed, are considered to be metastable. They are not found in nature nor have they been detected in hydrothermal equilibrium experiments.

*One pass of the spray gun over a specimen at 800°C was found to raise the specimen temperature momentarily to 1040°C. This is still too low a temperature to cause the transitional phase to transform to alpha alumina.

Erwin (13) suggested that the formation of the transition phases can be explained on the basis of the relative distribution of aluminum ions in the octahedral and tetrahedral interstices of a nearly cubic close-packed oxygen structure. For example, when boehmite ($Al_2O_3 \cdot H_2O$) loses water, the oxygen network supposedly forms quite readily, but the aluminum ions, which must reach their stable positions by diffusion through the oxygen framework, achieve this end to a varying degree depending on the heat treatment. The initial or lowest-heat-treatment form would have a random or at least a low-ordered distribution of aluminum ions with the distribution in subsequent phases becoming more ordered as the diffusion progressed. Further heat treatment of the last and most ordered transition phase would result in the aluminum ions reaching their stable positions, thus throwing the oxygen structure into a hexagonal closepacked configuration.

Plummer (14) has attempted to explain why the oxygen ions form a nearly closepacked cubic structure on first solidifying from the melt rather than going directly to the hexagonal closepacked structure which would result in the direct formation of alpha alumina. His explanation is based essentially on the formation in the cooling melt of small transient tetrahedral and octahedral groups of oxygen ions which arrange themselves in a certain order during solidification and on a postulated change in the coordination number of aluminum at high temperatures.

It would seem that Erwin's theory, which was developed to explain the structures observed during calcination of hydrated alumina, might also be applied to the structures formed during a rapid quench. In a severe quench there might be insufficient time for the aluminum ions to reach the equilibrium alpha-phase positions. This would result in the deposit crystallizing in a less well-ordered structure than alpha. The particle transition phase formed by the rapid cooling might well depend on the quenching rate. In this connection, Foster and coworkers (15) obtained delta alumina, a transition phase that is more ordered than eta or gamma, by quenching molten alumina under conditions which although not exactly described appear to have been less drastic than the conditions that exist when flame-sprayed particles strike a cold substrate. That extremely fast cooling occurs when a molten alumina particle strikes a cold surface is indicated by the computations described in Section X.

VII. PARTICLE FLUIDITY IN SPRAY

7.1 Glass slide sampling technique.

No satisfactory method was devised for measuring accurately the temperature of the small, high-speed particles. However, it was found that much could be learned about whether or not the droplets were above or below their melting temperature after any given travel distance by permitting the particles to strike the surface of glass microscope slides. They were mounted in an upright position at increasing distances from a rigidly fixed guide-rod, placed at the front of a spray-booth. In collecting a sample, the nozzle of the flame-spraying gun was placed on the guide-rod and the gun was moved manually across the booth at the rate of about three ft./sec. As the gun moved, the alumina particles struck each slide in turn and either adhered to the glass surface or bounced off, depending upon their condition at the instant of impact. The slides were examined subsequently with a microscope to determine how the adhering particles behaved on

impact. Because of the speed of gun movement during collection only a small number of particles were present on each slide.

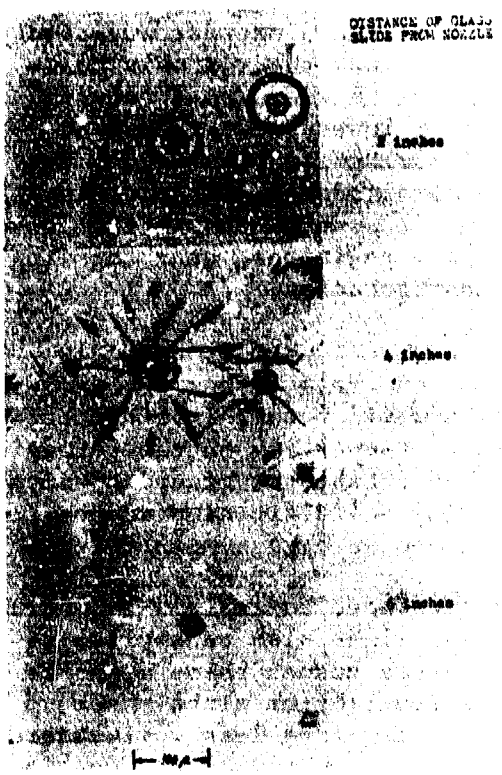

Figure 8. Appearance of alumina particles trapped on glass slides placed at different distances from the nozzle of powder gun B.

Figure 8 is typical of the appearance of alumina particles collected from the powder-gun spray. The two particles in Figure 8A were collected at 2 in. from the nozzle. Both have been flattened by the impact. Examination under polarized light showed the presence of alpha alumina, which is birefringent, in the center regions. The outer portion, however, consists of a non-birefringent or cubic type of alumina which has been shown to form whenever molten alumina is quenched rapidly. The presence of this cubic phase on the outer regions of the flattened particle, and the alpha alumina in the interior, strongly suggests that, at a distance of two inches from the nozzle, the two particles immediately before impact consisted of an envelope of molten alumina surrounding an unmelted core.

The flow patterns displayed by the particles in Figure 8B, together with a failure to detect the presence of any alpha alumina, constitute strong evidence that the particles had reached a completely molten condition after traveling 4 in. However, the droplets apparently cooled rapidly as they traveled beyond 4 in., because, at 6 in., the material that adhered was found to consist of slightly flattened spheres (see Fig. 8C). This observation implies that the droplets had cooled appreciably in only two inches of travel. Because of the temperature gradients incident to rapid cooling, the particles at this distance probably consisted of a solidified shell surrounding a molten core.

The particles collected on the glass slides in the early experiments gave a sampling of the many different particle sizes present in the spray. Subsequent tests of this type in which the various particle size fractions (see Section 5.3) were sprayed showed flow patterns comparable to those illustrated in Figure 8. Two observations of interest in these later tests were that (a) the large particles showed more radial flow on impact than the small ones, and (b) the large particles remained molten at greater distances from the nozzle than did the small ones. Further information on flow behavior of these particles is given in Section 8.3.

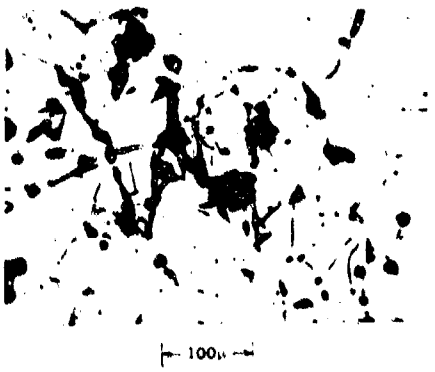

Figure 9. Appearance of alumina particles trapped on a glass slide placed 3 in. from the nozzle of the rod gun.

The typical appearance of slides on which particles from the rod gun had been collected is illustrated in Figure 9. The adhering fragments suggest a severe flow after impact. Flow of this type could be expected if the particles were molten at the instant of impact. Because of the relatively high velocity of the rod-gun particles, they travel much further in the same time interval than the powder-gun particles. This permits them to stay molten at greater distances from the nozzle. None of the particles from powder gun C were found to adhere at 16 in., yet a few particles from the rod gun adhered to glass slides at distances as great as 52 in.

7.2 Calculation of cooling rates of particles in spray

The derivation of expressions for computing the rate of solidification of a molten droplet travelling in a stream of hot gases is shown in Appendix II. A few sample computations were made using equations (4), (6), (7) and (8). Assumed values were 0.2 for the emittance of molten alumina and 2000°C for the melting temperature.

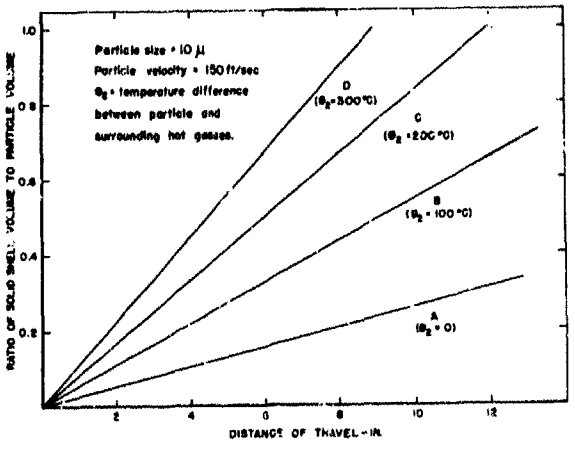

Figure 10. Computed solidification behavior of alumina particles.

The results of these computations are shown graphically in Figure 10. The particle diameter of 10μ and particle velocity of 150 ft./sec. are roughly comparable to the conditions obtained with a powder gun. Curve A indicates that if cooling of particles occurred by radiation only, a particle with a diameter of

10μ would be expected to travel some 3 or 4 ft. at 150 ft./sec. before solidifying completely.* However, observations with the glass slides showed that particles from both powder guns behaved as elastic solids and bounced away from the glass surface after only about 12 in. of travel. Curves B, C, and D show the computed volume ratios assuming cooling both by radiation and by convection to gases at temperatures 100, 200 and 300°C cooler than the particles. Comparison of these curves with the observed particle behavior indicates that the heat lost by radiation accounts for only a small part of the cooling and that a large temperature difference exists between the particles and the surrounding gas stream. No data could be found of temperatures in an oxy-acetylene flame. However, the turbulent nature of the flame suggests that there could be a considerable decrease in temperature at short distances from the nozzle.

VIII. FLOW BEHAVIOR AFTER IMPACT

8.1 Flow mechanisms of molten droplets

The appearance of the particles after striking a glass slide at normal spraying distances suggests that there was an appreciable radial flow after impact (see Fig. 8B and 9). Figure 8B, in particular, is of interest because of the evidence that the radial flow was channeled. Such a flow would be expected, from studies of droplets of a low-viscosity liquid striking solid surfaces (16). Further, when the terminal velocity of a droplet exceeds some critical value, a "splashing" effect is present. This splash effect is well-illustrated in Figure 11 which was taken by Edgerton (16) of a milk droplet striking a smooth metal surface. It is not difficult to visualize that the alumina particle illustrated in Fig. 8B passed through similar stages before solidifying.

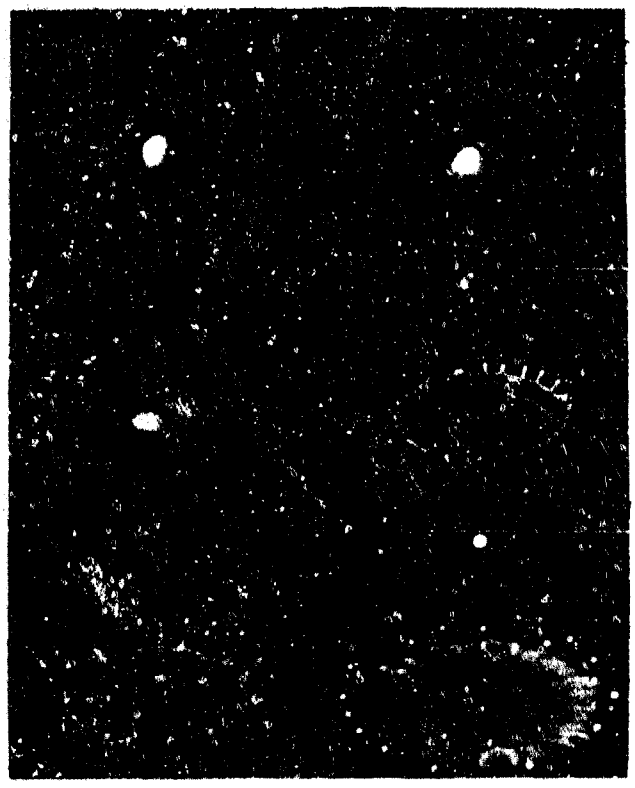

Figure 11. Sequence of high-speed photographs taken by Edgerton of a milk drop striking a flat plate. (Reproduced by permission of Charles T. Branford Company, Boston, Mass.)

*In the computations the particles were assumed to be molten when they left the nozzle which is not strictly true of powder gun operation.

When a drop that is molten, but travelling at high speed, strikes a cold smooth metal surface, there is a tendency for it to become atomized into finer fragments. Savic and Boult (18) have taken a series of high-speed photographs of a drop of molten paraffin, 0.5 cm. diam., striking such a surface. Figure 12 is a copy of their published sequence of photographs. They explain the observed atomization by assuming that that portion of the drop that first strikes the metal will solidify as it flows out radially. This leaves a thin, thermally-insulating layer of solidified drop material on the metal that is thinner near the center of impact than it is further out from the center. The geometry of this solidified layer forces the subsequent flow of residual molten material in the drop upward. This results in a torus of liquid moving up from the surface which, because of surface tension, breaks up into a myriad of tiny spheres.

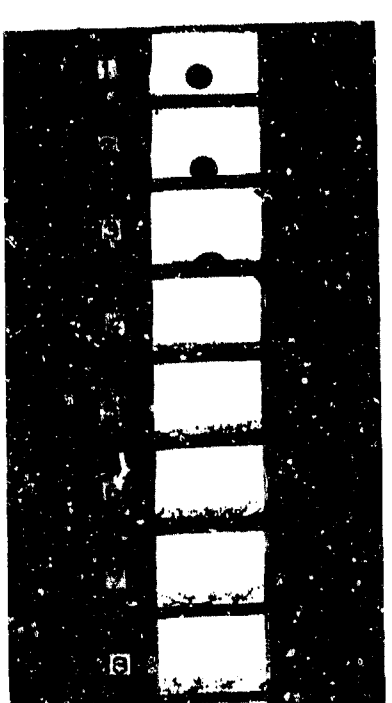

Figure 12. Drop of molten paraffin, 0.5 cm. diam., striking a cold metal surface. Sequence of pictures was taken by Savic and Boult (18).

There is some indication that a similar mechanism is active when molten alumina particles from the rod gun strike a polished metal surface, i. e., the impacting particle becomes atomized and the resulting small fragments are then carried away by the gas stream.* It was found, for example, that it was impossible to form a deposit on a cold specimen of polished platinum by spraying with the rod gun, yet when the same specimen was maintained at 650°C during spraying a deposit formed at what appeared to be a normal rate. It is possible that when the platinum was at 650°C, there was an insufficient quenching action to form the solidified layer near the center of impact and, without this layer the tendency for the strong upward movement of liquid would be absent; hence, there would be no atomization. Particles from the rod gun collected on polished platinum at 650°C had a somewhat similar appearance to those collected on glass slides at room temperature. As indicated in Section X the quenching rate when particles strike glass at room temperature is much lower than when they strike platinum.

Particles from the powder gun B were also sprayed on polished metal specimens. In this case, there was much less "atomization" on impact. Copper showed a minor amount; stainless steel almost none. The larger particles, after solidification on the metal, had a similar appearance to those on glass except that there was not as much radial flow indicated. The reason for this difference in behavior between the rod and powder gun particles is undoubtedly associated with differences in particle velocity. A high velocity is apparently required before the atomization effect becomes appreciable.

*The solidified residue would, if it stayed on the metal, act as an attachment point for a subsequent impacting particle. The observation that no layer formed on continued spraying suggests that the residue spalls off from the smooth metal as it cools.

8.2 High speed motion pictures of the impact of large drops of alumina.

Although numerous attempts were made to photograph the flow of flame-sprayed molten alumina particles on impact, these attempts were all unsuccessful principally because of the difficulties association with the small size and high velocity of the alumina particles. These difficulties are not present when larger droplets are used; hence, the only high-speed photographs of flow behavior that were obtained in the investigation came through use of molten alumina droplets with diameters of the order of ¼ in. In these tests, a metal surface was propelled at different velocities against a pendant drop of molten alumina that was formed at the end of 1/8 in. diam. alumina rod. A schematic drawing of the equipment is shown in Figure 13.

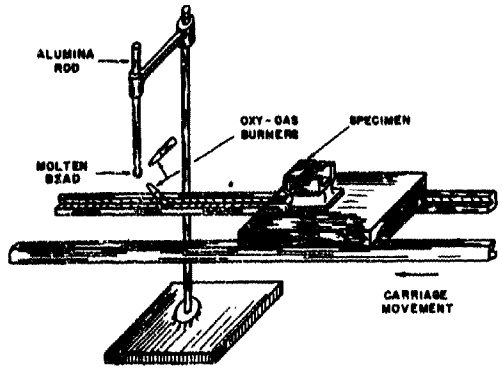

Figure 13. Schematic drawing of device used for striking a molten drop of alumina with a specimen moving at high velocity.

The metal specimen was attached to a carriage. This carriage was then propelled along a track that was 35 ft. long. The propelling force (up to 1000 lbs.) was applied by large high-tensile strength rubber bands. The carriage was released by a trigger mechanism. Upon release it travelled down the track and the specimen, mounted as shown in Figure 13, impacted the molten drop at the end of the tip of the alumina rod. Velocity of the carriage immediately before impact was measured by an electronic timer. The maximum velocity attainable with the equipment was 60 ft./sec. Stops of soft fiber insulation were placed at the end of the track to decelerate the carriage and bring it to a stop.

A sequence of photographs of the impact, which are typical of those that are obtained with an 8000 frame per sec. motion picture camera, are shown in Figure 14. The specimen speed was 29 ft./sec. The first few frames show the specimen approaching the drop. Impact, which occurs at frame no. 4 causes shattering of the molten alumina, and the resulting fragments travel rapidly away from the specimen (frames 4 to 21). The velocities of these fragments vary, but the fastest are travelling at about 90 ft./sec. or three times as fast as the impact velocity of the specimen. This increase in radial flow velocity over the impact velocity has been observed by Engle (17) for water drops.

The principle interest in the described experiment is in showing the type and degree of "atomization" that can occur on impact between cold metal and molten alumina. A somewhat comparable atomization is believed to occur when the small high-velocity, flame-sprayed particles from the rod gun strike a polished metal.

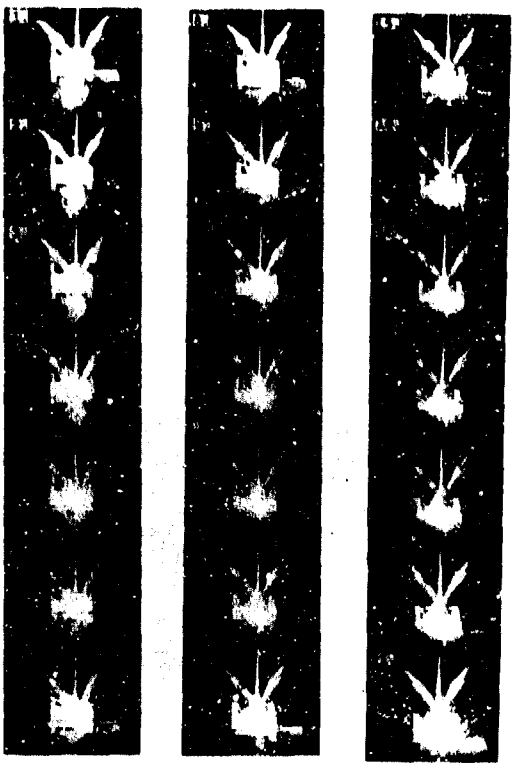

Figure 14. Sequence from a high-speed motion picture film showing collision between an iron specimen moving at 29 ft./sec. and a stationary drop of molten alumina. Specimen, which is moving toward camera, is visible as white strip immediately below burner tips. Drop of molten alumina in frames 1 through 3 does not register because its extreme brightness caused overexposure of film. Time interval between frames is approximately 0.5 millisec.

From the standpoint of the forming of real coatings, it is of course of greater interest to investigate the flow mechanism that occurs when the specimen is rough. However, photographing of large-drop impact on a "rough" surface was not attempted because of the difficulties involved in simulating a suitable large-scale model of a grit-blasted surface.

8.3 Flattening of powder-gun particles after impact

The effect of size on the flattening behavior of No. 105 alumina particles from powder gun C when they struck glass slides was investigated through use of the size fractions prepared as described in Section 5.3. Glass slides were first positioned at various distances from the gun nozzle. The gun was then moved rapidly in front of the slides after which the collected particles were examined with a microscope. The arithmetic average diameter of the flattened particles adhering to each slide was determined and this average was divided by the average particle diameter prior to spraying to give a "flattening ratio."

Figure 15 is typical of the results. The large particles (27μ) show a maximum flattening after a travel distance of about 5 in. The smaller particles, on the other hand, show a maximum after only 2 in. of travel. This picture is somewhat consistent with what might be expected from heat transfer considerations. The larger particles have greater mass than the smaller ones; hence, it would take a longer time in the flame (greater travel distance) for them to reach their optimum fluidity. A rigid theoretical treatment of the fluidity and flow for various particle sizes would be extremely complex and would require an

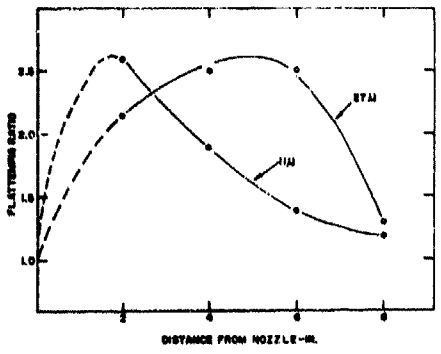

Figure 15. Effect of spraying distance on flattening behavior of alumina particles sprayed on glass with powder gun C.

exact knowledge of such particle parameters as heating and cooling rates in the spray, impact momentun, viscosity, surface energy, and quenching rates after impact.

IX. EFFECT OF SURFACE ROUGHNESS ON RATE OF COATING FORMATION ON GLASS AND COPPER

In Section 8.1 it was shown that high-speed particles of molten alumina become atomized on impacting a polished metal substrate. When the same particles strike a roughened surface a coating layer forms readily but the rate of formation, at least in the initial stages, is dependent on such variables as (a) the thermal conductivity and heat capacity of the substrate, (b) the substrate temperature, and (c) the degree of roughening. To determine how much these variables affected formation rate, a technique was developed for measuring quantitatively the rate at which the coating material was deposited on the substrate. This was done by passing the specimens at constant speed in front of the spray gun and measuring the gain-in-weight after each two passes. The specimens were small strips, 1 cm. wide by 4.6 cm. long, which were masked during spraying so that only an area of one $cm.^2$ was exposed to the impingement of particles. The specimens moved at a speed of 2-3/4 in./sec. during the spraying operation.

The weight of alumina deposited was converted to weight percentage of impinging particles that adhered to the substrate. To make this conversion, it was necessary to obtain the total weight of particles striking the test area. This weight was obtained through use of a collection cell consisting of a 50 ml. glass Erlenmeyer flask, the bottom of which had been reshaped into a cone with its apex pointing to the mouth opening. A mask having a 1 $cm.^2$ opening was placed at the mouth of the flask. The interior portions of the flask were coated with a layer of silicone grease. In collection of a sample, the particles passed through the 1-cm. opening, entered the mouth of the flask, and impinged on the cone-shaped bottom. Those that were not trapped by the silicone grease layer were deflected by the cone so as to rebound (at lower energy) into the grease layer on the inside walls. The collection efficiency of the cell was not determined but was estimated to be near 100%.

Blank determinations were made with no feed of alumina to the gun. A correction for weight loss of the silicone from the hot gases (which was small) was then made for each determination. No suitable technique was devised to give the weight loss caused by the trapping of hot particles by the silicone grease; however, the loss of volatiles from this heat source was believed to be considerably smaller than that caused by the hot gases.

The rod gun was used for all of these experiments, with a feed rate of 6½ in. per min. Figure 16 shows the percentage by weight of impinging alumina particles that adhered to glass microscope slides. At 3 in. from the nozzle, the glass surface was completely covered in three passes after which the weight of alumina deposited per pass remained constant; 86% of the impinging particles adhered. At 6 in., six passes were required to cover the surface; at 12 in. as many as 12 were required. The lower percentage of particles adhering with increased distance from the nozzle was probably caused by fewer particles being in a completely molten condition at the greater distance of travel (see Section 7.1).

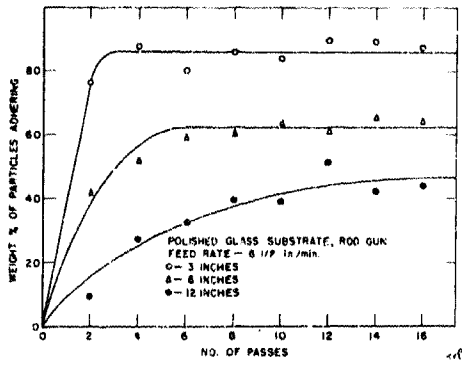

Figure 16. Weight percentage of alumina that adhered to glass slides placed at different distances from rod gun. Coating layer completely covered glass surface after 4 passes at 3 in., 6 passes at 6 in., and 12 passes at 12 in.

Figure 17 shows the effect of roughening the glass surface. The increase in percentage of the particles adhering to the rough surface as compared to the smooth surface was small and may not be significant, especially at greater than 8 passes.

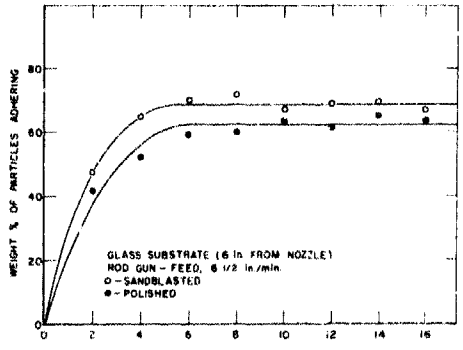

Figure 17. Effect of grit-blasting glass surface on the weight percentage of alumina particles that adhered.

Figure 18 illustrates the type of results obtained with a copper substrate. It will be noted that practically no alumina deposited on the polished copper. This result is in keeping with the findings observed with polished platinum. Roughening of the copper surface by blasting either with fine grit (No. 150) or coarse grit (No.60) permitted a layer to build up at a rate comparable to the rate obtained for a glass substrate. It is obvious from these results that severe "atomization" of particles (see Section 8.1) occurs only when the metal surface is highly polished. The curves suggest that a minor amount of this atomization occurs even on a roughened surface. However, once the surface is covered by a layer of coating material the rate of deposit is independent of the substrate material and the only factor that has any marked effect on the deposition rate at this stage is the distance of the specimen from the spray gun nozzle. Another observation of interest was that for sandblasted surfaces, the rate of deposition was largely independent of the substrate material, sandblasted glass giving approximately the same deposition rate as sandblasted copper.

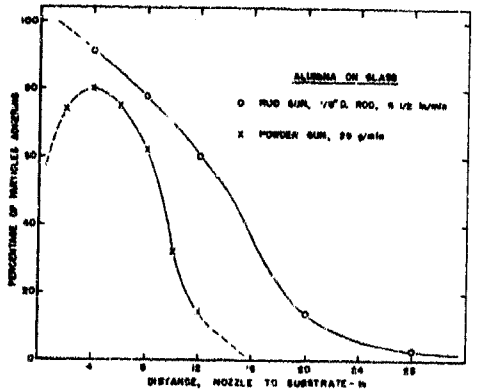

Figure 18. Effect of surface condition of copper specimens on percentage of alumina particles that adhered.

The aforementioned method of determining the percentage of particles adhering was unsuited for use with the powder guns because of their hot flames. This made it impossible to use the silicone-coated glass flask collection cell to obtain the weight of particles striking the test area. As an alternative, a second approach was used in which one half of a glass slide was smoked with carbon and the other half was left clean. The total number of particles striking the slide per unit area was determined by counting the rupture marks in the carbon film on the smoked area, and the total number adhering, by counting the particles per unit area adhering to the clean glass. This approach, while not as exact as the method described early, gave smooth curves for the percentage of particles (by number rather than by weight) that adhered to glass slides. The curves that were obtained are shown in Figure 19. Each value plotted is the average of two determinations.

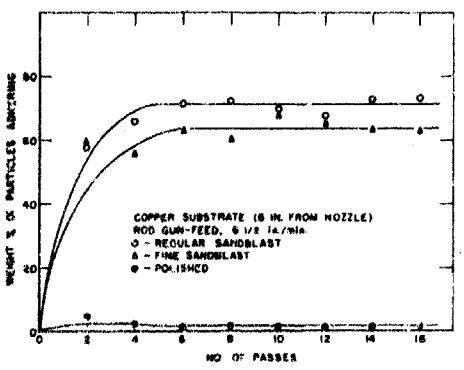

Figure 19. Percentage of particles by number from rod-gun A and powder-gun B that adhered to glass slides. Percentages were obtained by counts made on slides smoked with carbon (see text).

X. CALCULATION OF QUENCHING RATES

Heat transfer rates at the surface of a substrate being impacted by sprayed molten material is a complex, intractable problem involving heat sources such as the latent heat of freezing, heat generation from impact, and heat from the impinging hot gases. It is possible, however, to consider all of these contributions as a single heat source of small mass that is instantaneously applied to the substrate. This approach was used for the derivation given in Appendix III.

Programs for equations 2 and 3 in Appendix III were prepared for a digital computer and solutions were obtained for the conditions involved in spraying alumina on various substrates that were initially at room temperature. In these calculations, the kinetic energy transformed to heat on impact was assumed to be negligible; also the heat supplied by the impinging hot gases was not considered.

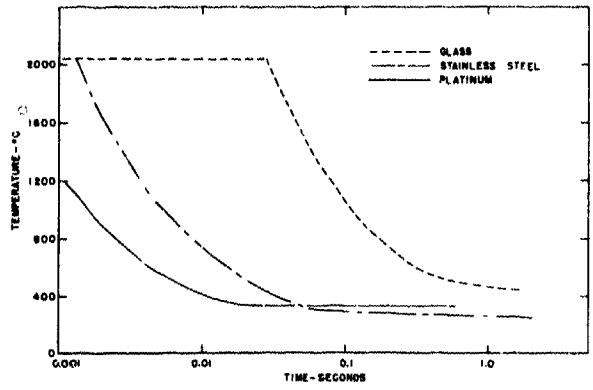

Figure 20. Computed time-temperature behavior when a 0.1 mm. thick layer of molten alumina is brought into contact with substrate materials at room temperature. Temperature is that of alumina layer next to substrate.

Figure 20 shows some of the results expressed as temperature-time curves for glass, stainless steel and platinum substrates. The thickness of the substrates was taken as 1 mm.; that of the alumina layer, 0.1 mm. The temperature was computed for the interface. According to the curve for stainless steel, the computed temperature of the alumina near the interface decreases from 2050°C to 1800°C at an average cooling rate of 800,000°C/sec. while the cooling rate on glass is 34,000°C/sec. The curve for platinum was not computed for times shorter than 0.001 sec. but from its position in Figure 20 a cooling rate much higher than stainless steel would be expected.

The high-speed cinecamera pictures also indicated extremely rapid quenching rates on impact. For example, the molten particles from the rod gun emitted sufficient radiation to expose the film strongly just before impact upon a previously applied coating layer; yet about 0.5 milliseconds after impact the particles had cooled to such an extent that they were no longer visible on the film.

The computed curves of Figure 20 are helpful in predicting the flow behavior of the particles on striking various substrates. The upper curve indicates that a small mass of molten alumina striking a glass surface can be expected to stay molten and presumably flow for about 0.03 sec. The same mass striking stainless steel would solidify in about 0.001 sec. and for platinum the time would be even shorter. In the calculations, it was assumed that the alumina was at its melting point on impact, and that it gave all of its latent heat of fusion upon solidifi-

cation at the same temperature. Most of the latent heat is absorbed by the substrate and the computed differences in time required for solidification (see Fig. 20) result from differences in thermal conductivity and heat capacity of the substrate material.

XI. BOND STUDIES

The mechanisms responsible for the bonding of flame-sprayed alumina to metals were studied by (a) measuring the apparent bond strength in both shear and tension of coatings that had been applied to iron specimens with controlled surface roughnesses, (b) evaluating the effect of oxide films on bond development to smooth metal surfaces, and (c) determining the effect of surface roughness on the oxidation behavior of iron specimens.

11.1 Shear tests

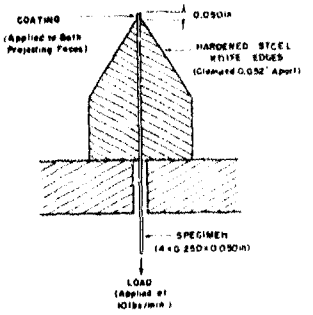

Figure 21. Arrangements for shear tests

The arrangement for determining bond strength in shear is shown schematically in Figure 21. The equipment was designed so that five specimens surface ground to a thickness of 0.050 in. and a width of 0.250 in., could be mounted between two hardened steel blocks which are shown as an end view in the figure.

All of the tests were made with ingot iron specimens. One set of specimens was left in the surface ground condition; other sets (6 specimens each) were subjected to different grit-blasting treatments that imparted different degrees of roughness. No. 60 silicon carbide grain was used as the abrasive. The conditions selected to impart the varying degrees of roughness are listed in Table 8.

In preparing for a test, the set of six specimens were first placed in a jig that would shield all but a 0.050-in. length at the upper end of the specimen. After both faces had been subjected to the selected blasting treatment, the jig was removed and five of the specimens were clamped into position in the shear-test equipment (Fig. 21). The equipment was then placed on a specially constructed table that was mechanically moved back and forth in front of the flame-spray gun. The table was designed so as to cycle at any of several constant rates. The spraying, which was done with the specimens at normal spraying distance and with a table movement of 2-3/4 in. per second, was continued until the thickness of the coating layer on the tips of the specimens projecting above the two hardened steel blocks was 0.010 ± .001 inch.

TABLE 8.

CONDITIONS USED FOR IMPARTING DIFFERENT DEGREES OF SURFACE ROUGHNESS TO INGOT IRON SPECIMENS

Treatment No.	Description of Treatment	Blasting Conditions			
		Abras.	Dist.[a]	Air Press.	No. of Passes
			in.	psi	
1	Very light blast	SiC[b]	7	40	4
2	Light blast	"	7	60	8
3	Medium blast	"	4	75	4
4	Strong blast	"	4	80	10
5	Heavy blast	"	2	80	15

a/ From nozzle to surface of specimen
b/ No. 60 grit.

After application of the coating, the equipment was removed from the reciprocating table and the force required to shear the metal from the coating shell was determined. This was done by attaching a bucket to each specimen in turn and feeding small lead shot into it at a constant rate of 500 psi/min. until the coating layer was sheared from the metal. When failure occurred the specimen slipped through the hardened-steel blocks and the resulting movement actuated a cut-off switch that stopped the flow of the lead shot. The weight of the bucket and lead shot upon failure of the specimen was determined, and this weight was divided by the area of surface that was coated, to obtain the apparent shear strength of the bond. In nearly all cases, the coating layers came off of both faces at the moment of failure, leaving clean metal surfaces; when this type of failure did not occur, the determination was not considered reliable, and the value was not included in the data.

The sixth specimen that had been subjected to the blasting treatment was not flame sprayed. Instead, it was plated with nickel by the electroless process (19) to preserve the contour, sectioned, and examined with a metallographic microscope. Photomicrographs were taken of five randomly selected fields at a magnification of 315X, and projected on white paper with a further enlargement of 12X*. The contour of each projected interface was then traced on the paper, as shown in the illustration below. The length of the contour line BB was determined with a map measure; the straight line distance AA with a ruler.

The percentage increase in surface area was then taken as: $\frac{BB^2 - AA^2}{AA^2} \times 100$.

*The degree of roughening observed after the various treatments is somewhat dependent upon the resolving power of the magnification system. At very high magnification, micro-deviations can be detected that are not visible at 300X. At such magnifications, measurement of a prohibitively large number of fields would have been required to obtain representative average values.

TABLE 9.

APPARENT BOND STRENGTHS IN SHEAR OF
FLAME-SPRAYED COATINGS OF ALUMINA APPLIED AT A THICKNESS OF 0.010"
TO INGOT IRON SPECIMENS HAVING DIFFERENT SURFACE PRETREATMENTS

Surface Treatment No.	Description of Surface Treatment	Increase in Surface Area[a] %	Powder Gun-5" from Nozzle			Rod-gun-3" from Nozzle		
			No. of Spec.	Avg. Shear Strength psi	Coef. of Var.[b]	No. of Spec.	Avg. Shear Strength psi	Coef. of Var.[b]
0	Surface ground	1.2	1	0[c]	0	1	[d]	-
1	Very light blast	18.0	5	0[c]	0	3	381	32.6
2	Light blast	25.5	5	0[c]	0	5	673	19.2
2B	Light blast-Ox. 300°C	25.5	-	-	-	5	733	38.0
3	Medium blast	33.7	5	682	24.5	8	2275	17.5
4	Strong blast	40.2	5	1015	17.3	3	3415	19.6
4B	Strong blast-Ox. 300°C	40.2	4	1377	4.4	-	-	-
5	Heavy blast	41.7	5	1696	32.2	-	-	-

a/ Determined for uncoated specimens - see text.
b/ Coefficient of variation = $\frac{\text{Standard deviation}}{\text{Avg. shear strength}}$ (100).

c/ Coating came off on cooling.
d/ Impossible to form coating layer.

The results, which are given in Table 9 and Figure 22, can be summarized as follows:

(1) The bond strength of alumina coatings to ingot iron as measured by the described procedure increased exponentially with increasing surface roughness.

(2) Coatings applied by the rod gun developed significantly stronger bonds than those applied by the powder gun.

(3) Preoxidizing for 1 hr. at 300°C in air prior to flame spraying had little effect on the determined shear strengths.

The observation that the shear strength increases with increasing surface roughness implies that the bond may be mostly mechanical. The surface area of the specimen of course increases with increased roughness but, if the bond was entirely chemical, the strength of the bond should increase linearly with surface area. Figure 22 suggests that the relationship is not linear but that it is more exponential in nature.

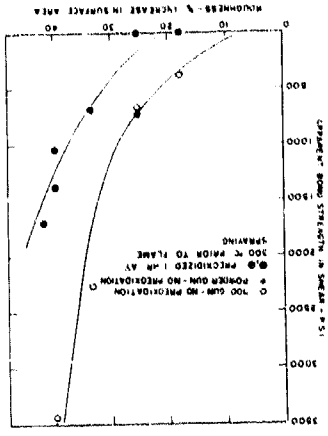

Figure 22. Effect of surface roughness on apparent bond strength in shear between ingot iron and alumina coatings applied with rod gun and powder gun B.

On a well roughened surface, failure of the bond in a shear test probably cannot occur without some fracture of the coating material. This concept is illustrated by the following sketch in which AA' is the line of fracture.

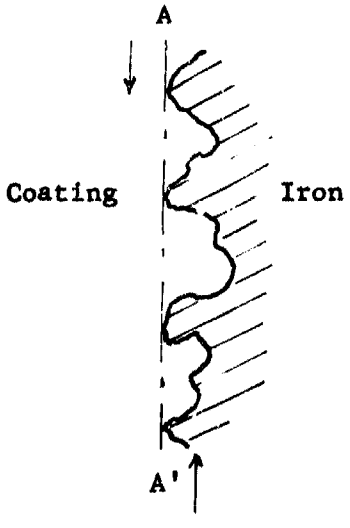

If such a mechanism is active, then the rod-type coating which should possess a stronger structure than the powder gun coating because of fewer pores, would give the higher shear-strength values. Figure 22 shows that such is the case.

11.2 Tensile Tests

A few measurements were made of the bond strengths in tension of powder gun B coatings applied to low-carbon steel specimens. The test procedure was similar to that used by Brown (20) and Shepard (21). The specimens were cylinders, 1" diam. by 9/16" long. The annular surface at the end of each specimen was roughened by controlled grit blasting, after which a layer of alumina about 0.020" thick was applied with powder gun B. After cooling, the thickness of the coating was reduced to 0.010" by surface grinding with a diamond wheel. Next, one

drop of Eastman 910 adhesive* was applied to the coating surfa e. A second cylinder of the same diameter, and with a machined and lightly grit-blasted surface, was then placed over the coated surface of the first cylinder. The two cylinders were aligned carefully and then pressed together at room temperature for 30 min. with a force of 100 lbs. Finally, the bonded specimen was attached through universal joints to the heads of a tensile testing machine and the joint tested to failure at a loading rate of 600 lbs. per min.

The results are given in Table 10. In most cases, fracture occurred at the metal-coating interface. When fracture occurred elsewhere, the determination was disregarded on the grounds that the test did not measure the bond strength of the interface under study.

TABLE 10.

APPARENT BOND STRENGTHS IN TENSION OF POWDER-GUN COATING B APPLIED TO LOW-CARBON STEEL CYLINDERS, 1" DIAMETER.

Specimen No.	Surface Treatment	Apparent Strength of Bond
1H	Heavy grit blast	382 psi
2H	" " "	435
3H	" " "	356
4H	" " "	379
5H	" " "	433
6H	" " "	478
7H	" " "	408
8H	" " "	408
	Average -	409.9
	Coefficient of variation[a/] -	8.9%
1L	Light grit blast	279
2L	" " "	274
3L	" " "	284
4L	" " "	324
5L	" " "	248
6L	" " "	242
7L	" " "	369
8L	" " "	274
	Average -	287.7
	Coefficient of variation[a/] -	13.5%

a/ Ratio of standard deviation to average strength when expressed as percentage.

*Available from Armstrong Cork Company. Ind'l. Adhesive Sales Div., Lancaster, Pa.

A comparison of the bond strengths in tension (Table 10) with the bond strengths in shear obtained on comparable surfaces (Table 9) indicates that the shear strengths are higher by a factor of about 2.5. This ratio in strengths is in good agreement with that observed for grit-blasted cold-rolled steel specimens sprayed with steel metal from a wire gun (5).

Because of the time-consuming nature of the tensile tests, no attempt was made to establish a quantitative relationship between roughness and bond of the type illustrated for the shear tests in Figure 22. However, the results listed in Table 10 are clear in showing that there is a very appreciable increase in the tensile strength of the bond with an increased surface roughness.

11.3 Bond to smooth surfaces

Although many trials were made, no measurable bond was ever achieved on a smooth metal surface. With a smooth glass surface, however, good bond developed readily. This was demonstrated by applying a porcelain enamel ground coat (a low melting silica glass) to the face surfaces of ingot iron tensile test cylinders. The enamel, after firing, had the normal smooth, fire-polished surface. An alumina coating was applied to this surface with powder gun B and the strengths in tension determined as described in Sec. 11.2. The average strength for five specimens was 672 psi; the coefficient of variation was 15%. In no case did failure occur at the glass-alumina interface; instead, the fractures occurred in the alumina coating.

Because the strong bond to glass might possibly be caused by the relatively slow cooling rate of the molten alumina particles after they strike the glass surface (see Sect. X), thereby permitting more time for reaction than when they strike metal, an experiment was performed in which an alumina coating was sprayed on a thin metal film. This film was formed by first impregnating with copper a 0.004 in. thick layer of porcelain enamel that had been previously applied to tensile test specimens. This was done by moving a high-speed, copper-impregnated steel brush over the enamel surface. This treatment resulted in a thin and adherent film of copper which was sufficiently conductive to be used as a base for electroplating. Nickel was electroplated over this film to a thickness of 0.0003 in. and, finally, alumina was applied with powder gun B to the smooth nickel surface to a thickness of about 0.010 in. In two of three trials the flame-sprayed alumina parted from the nickel film on cooling. In the third case, the alumina remained on the specimen but the bond strength was so weak that the coating parted from the nickel film while it was being attached to the tensile test cylinder.

The possibility that adherent oxide films on smooth metal surfaces might permit bond development was also investigated. Ingot iron specimens were used for this work. The oxide layers formed by preheating in air were found earlier to have little effect on bond (see Fig. 22). It seemed conceivable, however, that under flame-spraying conditions where the metal surface was heated by a flame high in moisture content, the formation of an iron-rich film might be favored. Such layers when formed in steam in the range 700° - 1100°C are reported to be strongly adherent (22).

To determine whether or not a layer of this type would increase the bond strength of a flame-sprayed coating, a number of shear-test specimens were first surface ground to give a smooth finish and then oxidized for varying times in steam at 800°C. Four treatment times were selected: 2, 4, 8 and 16 min. The oxide layers formed by all four treatments had a smooth, dark gray appearance and they were tightly adherent to the metal. Sections through the oxide gave no evidence of a layer structure (see Fig. 23) such as is normally observed when more than one of the oxides of iron is present (22) and, in addition, x-ray diffraction patterns obtained with a cobalt target showed lines for only wüstite (ferrous oxide) and iron.

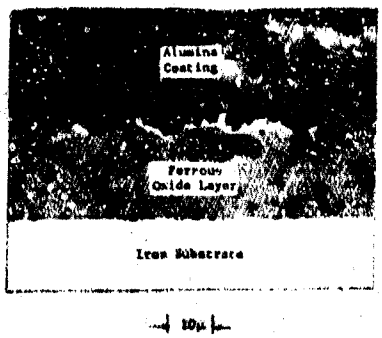

Figure 23. Micrograph of ingot iron specimen that had been oxidized in steam for 8 min. at 800°C and then coated with alumina by powder gun B.

The average bond strengths in shear of powder-gun coatings of alumina (gun B) that was applied to the treated specimens having different thicknesses of FeO are plotted against film thickness in Fig. 24.

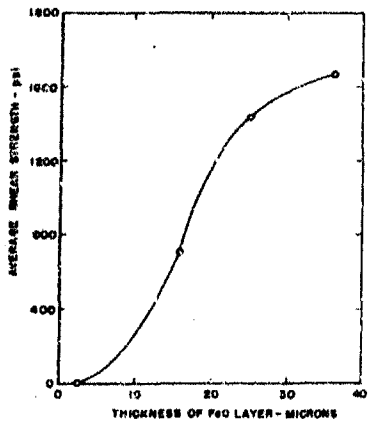

Figure 24. Effect of thickness of FeO layer on apparent shear strength of bond between ingot iron and on alumina coating applied with powder gun B.

The average shear strength of surface-ground specimens preoxidized for 16 min. in steam at 800°C was 1662 psi. This value compares to a shear strength of 1696 psi for specimens that had been given a severe roughening treatment but that had not been preoxidized (see Table 9). Thus both surface treatments yielded approximately the same bond strength when determined by the shear test.

The smoothness of the iron surface (see Fig. 23) rules out any appreciable mechanical interlock between the iron and the ferrous oxide layer. The coating-ferrous oxide interface, on the other hand, is highly irregular and some mechanical gripping between coating and oxide is indicated. The oxide on specimens oxidized for only 2 min. in steam (layer thickness 2.5μ) was free of these surface irregularities and, as shown in Fig. 24, the specimens showed no measurable shear strength.

As an additional confirmation that the roughness at the outer layer of oxide was contributing to the bond, bond strengths in tension were measured for two groups of ingot iron specimens that had been oxidized in steam and then coated with alumina with powder gun B. The specimens consisted of cylinders, 3/4 in. diam. by 1 in. long, with one end threaded for attachment to the grips of the tensile machine. The opposite end of each cylinder was surface ground after which the specimen was oxidized in steam for 15 min. at 800°C. This treatment gave an FeO layer, 59μ thick, on the surface-ground face. The outer surface of this layer was rough and irregular.

In the first tests, the alumina coating was sprayed directly onto this roughened oxide; the average tensile strength for six specimens was 870 psi. In the second tests, the oxide layer on the specimen face was ground and then given a high polish prior to application of the coating; the thickness of the layer after this treatment was about 38μ. Three specimens with this polished oxide were flame-sprayed with powder gun B. On two of the three, the coating separated from the oxide layer before the tensile test could be made. On the third, the coating remained on the specimen and a bond strength of 102 psi was measured. Failure occurred at the interface between the polished oxide and the coating. Examination of this interface with a microscope after failure showed that the adjacent areas represented spots where the larger particles in the spray had struck the surface. Thus, because of the slow cooling of the large mass, it is conceivable that, at least at these spots, there was sufficient time at high temperature for the formation of an iron-alumina spinel at the interface. Such reaction, which has been postulated by Meyer (8), would, of course, lead to a strong chemical bond.

11.4 Effect of surface roughness on the oxidation rate of iron

It was shown in an earlier study (23) that grit-blasted iron oxidized at a slower rate than iron that had not been grit blasted. Thus, it appeared possible that either the type or quantity of oxide on a roughened surface was different than on a smooth one and that it was this difference in oxide rather than in roughness, per se, that was responsible for the observed differences in bonding behavior. It thus became one of the major goals of the study on bonding to determine why a roughened surface of iron, in spite of its larger gross surface area, oxidized at a lower rate than a smooth one.

The results of this separate phase investigation are of considerable interest in the field of oxidation research and they will be published in a separate paper (24). The major findings are listed as follows:

(a) By a severe roughening of the surface of ingot iron, the oxidation rate in air at 800°C was reduced by a factor of 6.

(b) The reduction in rate was directly proportional to the degree of roughening.

(c) The reduction was associated with differences in surface geometry and not with contamination by grit materials.

(d) The cause of the reduction was the formation of small voids in the oxide that grows on rough surfaces. These voids, in turn, act as diffusion barriers which inhibit the flow of iron ions outward and thereby lower the rate of oxide formation. The voids are formed by local stresses in the oxide. The stresses are present on rough surfaces but not on smooth ones.

(e) No voids appeared in the oxide on a smooth surface until such time as the ingot iron surface became roughened by preferential oxidation effects. This roughening was not observed for a highly purified iron (99.999 Fe).

These findings, while of considerable general interest, did not contribute in a positive way to explaining why a superior bond developes when alumina is flame sprayed on a roughened metal surface.

11.5 Discussion of bond mechanism

All of the evidence from the aforementioned experiments indicate quite strongly that the bond of flame-sprayed alumina to metal is mostly mechanical. If the bond was chemical then some bonding would be expected on a smooth iron surface and the strength of this bond would be expected to increase linearly with increase in surface area as the metal was roughened. That such is not the case is shown by the shear test results (Fig. 22). Also, the results of the tension tests showed that no measurable bond developed on a smooth iron surface.

The results of the one test with a smooth layer of ferrous oxide indicates that bond can be developed to an adherent oxide if the quenching rate of the alumina particles after impact is not too rapid. On a grit blasted specimen asperities project up from the surface. A molten particle striking one of these asperities would be expected to cool more slowly than if it were to strike a smooth flat area. If one assumes the asperity to have an adherent oxide, then it would be possible for a spinel to form which would supply the chemical bonding. However, the experiment with the thin nickel layer applied over glass suggests that even with relatively slow cooling rates good bond does not develop. Tylecote (25) has shown that an extremely adherent oxide film forms on a smooth nickel surface; hence, the lack of bond to the thin electrodeposit of nickel probably cannot be ascribed to the lack of an adherent oxide film.

Meyer (8) concluded that the bond of flame-sprayed alumina to metal is mostly mechanical. Even for most sprayed metal coatings, good bond occurs only on rough irregular surfaces and according to Ingham and Shepard (5) the bond that develops between the coating and the metal in ordinary metallizing is almost entirely mechanical in nature.

The stresses present at the coating metal interface are a critical factor in determining whether or not a coating will remain on a metal surface. Consider molten droplets striking a cold, rough surface of metal. The droplets deform on impact and become interlocked with the mechanical projections and indentations in the metal. The alumina shrinks during solidification and cooling while the adjacent metal, which is absorbing heat from the alumina, expands. This process places the alumina in tension. Later, when the coating operation is completed and the specimen is cooled to room temperature, the metal, which in most cases has a higher expansion coefficient that the alumina, undergoes more shrinkage than the coating. Thus, the alumina, after cooling, is wedged into the surface irregularities of the metal by compressive forces and is thereby capable of withstanding the room temperature and shearing stresses that tend to separate the coating from the metal. On a smooth metal surface, there is no "keying-in" action and unless a very strong chemical bond develops, the coating will separate from the metal on cooling. The observation that such a separation occurred in all tests on smooth untreated metals, either immediately on cooling or before a bond test could be completed, shows that if a chemical bond existed on any of the smooth untreated metals it was insufficient of itself to resist the shearing stresses that existed at the interface.

XII. INVESTIGATION OF STRESSES

As pointed out in the preceding section, the stresses present at the interface between a particle-impact coating and a metal substrate sometimes exert a controlling influence on whether or not the coating will remain on the metal. These stresses are complex in origin because the coating does not solidify homogeneously, but rather droplet by droplet in successive layers. This method of formation introduces stress gradients within the coating layer and makes a rigid stress analysis extremely difficult. Attempts were made to arrive at such an analysis but these were unrewarding mostly because of the necessity of introducing questionable assumptions.

Equipment for measuring deflections (and, indirectly, stresses) in coated strip specimens at various temperatures was constructed and used for a few preliminary measurements before the program was terminated. Fig. 25 shows this equipment. As may be seen in the photograph, the ½ in. wide by 6 in. long 24-gage specimen was coated on one side over an area about 3 in. long. During measurement the specimen was supported at its top in the apparatus by a Nichrome rod which was fastened to the base-plate.

Attached to the bottom of the specimen was a pointer of very small mass. The pointer extended down through a slit in the base-plate.

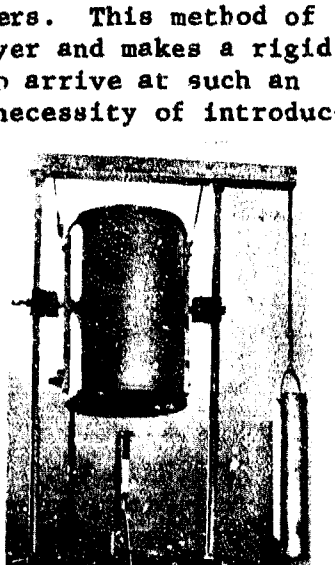

Figure 25. Stress analysis equipment.

Due to the differences in the thermal expansions of the coating and metal, the coated area acted as a bimetallic strip when the specimen was heated, causing a deflection of the pointer. The experimental procedure consisted of determining this deflection at various temperatures with a cathetometer. The pointer deflection was used to calculate the radius of curvature of the coated area of the specimen. The stress occurring at the coating-metal interface could then be determined if the moduli of elasticity of the coating material and the base metal were known at the temperature of interest.

The complete procedure for determining the interfacial stresses occurring in a specimen at various temperatures was as follows:

The specimen blank was first prepared for coating by blasting the surface with No. 60 alumina grit at an air pressure of 80 psi. The V-shaped pointer was then spot welded to the bottom of the specimen blank; a chromel-alumel thermocouple, made of 3-mil wires wound as a helix to offer as little resistance as possible to movement, was attached; and the assembly was placed in the apparatus. The specimen was then removed and placed in a special coating jig which supported the specimen at one end during coating so that it was free to flex or change shape without restraint. The specimen was coated with the rod gun by a mechanized operation on the front side over a 3 in. long area. It was then removed from the coating jig, put back into the apparatus and the pointer position again determined. The difference between the pointer position before coating and the position after coating was taken as the deflection caused by the coating procedure.

For obtaining deflection values at elevated temperatures, the counterbalanced, resistance-heated furnace was lowered about the specimen and heated at a rate of 3°C per minute. A typical pointer deflection vs temperature plot for a specimen coated with the rod gun is shown in Figure 26.

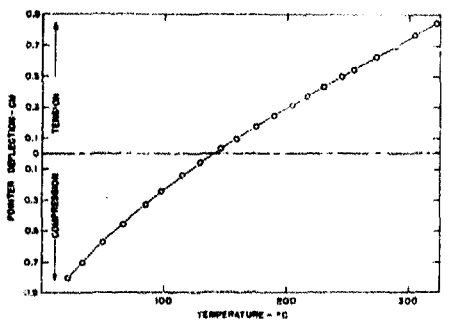

Figure 26. Effect of temperature on deflection of ingot iron strip coated with rod-gun alumina on one side.

Because the specimen coated on one side only acts as a bimetallic strip, the following relationship developed by Timoshenko (26) can be applied:

$$S_i = \frac{1}{R}\left[\frac{2}{t_c t_h}\left(E_c I_c + E_m I_m\right) + \frac{E_c t_c}{2}\right]$$

Where:

R = Radius of curvature of strip
S_i = Stress at the interface
t_c = Coating thickness
t_h = Specimen thickness (coating plus metal)
E_c = Modulus of elasticity of the coating material
E_m = Modulus of elasticity of the metal
I_c = Moment of inertia of the coating
I_m = Moment of inertia of the metal

Ault (1) gives values for the room-temperature moduli of elasticity of a rod gun alumina coating of 6.1 and 6.6 x 10^6 psi for two specimens. Using the mean of these two values, the compressive stress in the coating for the specimen for which the deflection data are given in Fig. 26, was computed to be 1500 psi.

Figure 27 shows the effect of coating thickness on the curvature of specimens measured at room temperature. Curve (a) shows that the curvature of 24-ingot iron specimens coated on one side only increases with increasing coating thickness. The negative curvature signifies that the coating was on the convex side of the specimen.

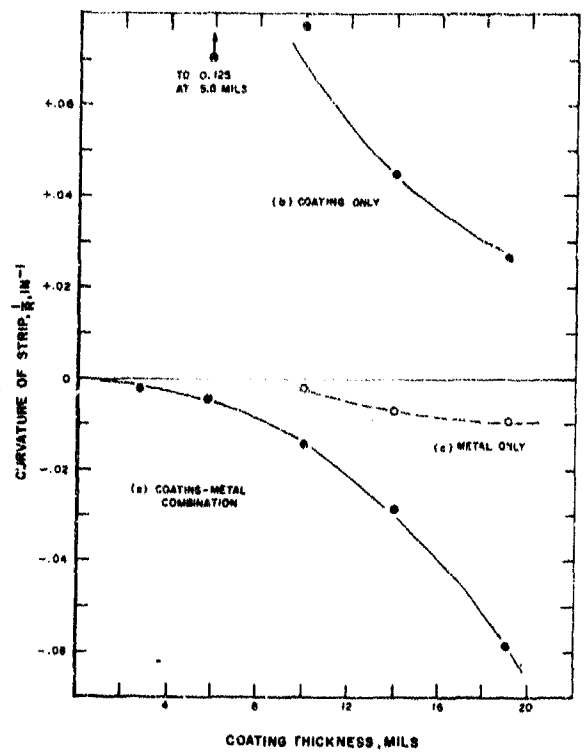

Figure 27. Curvature of strips with thickness. (Negative curvature values in curve (a) signifies coating was on convex side of specimen).

After the points for curve (a) were determined, the coating layers were removed from the ingot iron by completely immersing the specimens in 20% sulphuric acid at room temperature for approximately one hour. The coating and the iron backing separated cleanly during this treatment with no cracking of the coating layer. The alumina coating showed no attack by the acid; the loss in thickness of the iron was less than 0.5 mil.

The coating strips assumed a reverse curvature on parting from the metal. These curvatures were measured and are plotted as curve (b) in Fig. 27. The reverse curvature shows that an internal stress gradient is still present in the coating after separation, the side that was originally next to the metal being in compression and the outer surface in tension. This stress gradient can be explained on the basis that during application of the coating, molten alumina impinges and solidifies on an earlier sprayed layer that has already partially cooled.

Curve (c) for "metal only" in Fig. 27 shows that some of the iron specimens retained a "negative" curvature after the coating was removed. This indicates that the ingot iron was permanently deformed. This deformation was observed, however, only when relatively thick coatings were applied.

XIII. CONCLUDING REMARKS

Although a complete understanding of all of the various facets of the particle-impact process was not achieved during the course of the investigation, the study did result in an improved knowledge of some of the mechanisms that are active when alumina is flame sprayed on a substrate. In this section of the report an attempt is made to summarize the more important findings of the study, and at the same time to present what the authors believe to be some of the more probable mechanisms of the flame spraying process.

Powder-gun spraying. In powder gun spraying a particle begins to melt soon after it enters the flame. Other things being equal, the time in the flame required for complete melting of an individual particle depends on its diameter. For powder gun B, dwell-times of the order of 0.003 sec. are required for complete melting of the average size particle. This corresponds to a spraying distance of 5 in. The particles cool rapidly as they travel further downstream. The particles do not agglomerate in the flame but instead maintain their original identity.

The peak velocity reached by particles 11μ in diam., when sprayed with powder gun C, was 203 ft./sec. (3 in. from nozzle); by 17μ particles, 196 ft./sec. (3 in. from nozzle), and by 26μ particles, 138 ft./sec. (6 in. from nozzle).

Rod-gun spraying. Melting takes place in the rod gun at the tip of the rod as it is fed at a constant rate into the flame. The molten material is apparently held at the rod tip until the force exerted by the surrounding gas stream exceeds the surface tension force of the molten alumina. When this condition is reached, the molten material is torn away from the rod tip and atomized, after which the process is repeated. This results in bursts of particles, rather than a continuous spray. High-speed motion pictures showed that with a 1/8 in. rod the percentage of time that rod-gun A was spraying particles varied from 3% for a feed rate of 2 in./min. to 40% for a feed rate of 8 in./min.

The particles from the rod gun undergo a rapid acceleration for the first 2 in. of travel to a peak velocity of some 600 ft./sec. after which they begin to decelerate. Although cooling rates in the spray are faster for rod-gun than for powder-gun particles, the rod gun particles, because of their higher velocity, travel greater distances before they solidify. A few of the rod-gun particles were found to be molten after travel distances of as great as 52 in.

Flow behavior after impact. The molten particles undergo severe deformation and radial flow after impact on a smooth surface. For the relatively low velocity powder-gun particles, this flow sometimes resembles that of a water drop striking a smooth plate. At higher velocities (rod gun spraying) the molten droplets become atomized into smaller particles after impact on a smooth metal. This is probably caused by a peripheral freezing around the outer area of contact, followed by an outward flow of the remaining molten material. On rough surfaces, however, there is very little atomization and much less radial flow.

The molten droplets undergo a severe quenching action when they strike a substrate. Heat transfer calculations indicate that a layer of molten alumina 0.1 mm thick would stay molten for only about 0.001 sec. when brought into contact with a 1-mm. substrate of stainless steel; on glass, the same mass of alumina would stay molten for approximately 0.03 sec.

The percentage of particles that adhere after impact normal to the substrate surface is dependent on (a) the geometry of the substrate surface, (b) the thermal properties of the substrate, and (c) the size, velocity, and temperature of the droplets. Once a layer has formed, however, the percentage of newly arriving particles that adhere is largely independent of the original substrate.

Crystallinity. Probably because of the high quenching rates on impact, the alumina crystallizes in a metastable form rather than as alpha alumina. The metastable phase was identified as eta alumina. This deposited material was found to have a microhardness lower than that of either a single-crystal alpha alumina (sapphire) or a sintered alpha alumina body.

Stresses. An alumina layer flame-sprayed on iron (or on other metals with equal or higher expansion coefficients) is under compression at room temperature. This compression attenuates on heating and changes to tension at higher temperature. A residual stress gradient was found to exist in the coating layer after its removal from the metal; the alumina layer that was originally next to the metal was in compression and the outer layer was in tension.

Bond. When molten particles strike a rough metal surface, they conform with the indentations and projections of the metal. This gives a "keying-in" action that permits the coating layer to withstand the shear stresses that develop at the interface on cooling.

Chemical bond sufficient to withstand the interfacial shear stresses was developed on a smooth glass surface but it was never achieved on a smooth metal. Strong bonds were obtained by flame spraying onto an adherent ferrous oxide film formed by oxidizing smooth iron specimens in steam. When the rough outer surface of the ferrous oxide layer was polished prior to flame spraying, however, the alumina coating no longer adhered.

A weak chemical bond may form between oxide films present on metal surfaces and the sprayed alumina layer; however, this bond must be supplemented with a mechanical keying action to survive the shearing stresses that develop at the interface.

XIV. RECOMMENDATIONS FOR FURTHER WORK

Further study in several areas is indicated before a completely satisfactory understanding of the particle-impact process will be possible. Four areas in which additional work is indicated are the following:

(1) Plasma-jet spraying. Flame-spray guns operate satisfactorily only in narrow ranges of gas flow and material feed rates. It is difficult if not impossible with guns of the types used in this study to achieve significant variations in particle velocities and particle temperatures. If these factors could be varied, while the particle size is held constant, it should then be possible to study independently the effect of both temperature and velocity on the flow behavior of the particles after impact, and also to investigate how variations in the temperature and velocity of particles affect the coating structure. The plasma-jet should be a versatile tool for a study of this type. It should be possible with a suitable plasma-jet (a) to vary particle temperature by varying the power input and (b) to vary particle velocity over a reasonably wide range by varying the gas flow rates.

(2) Formation of coating consisting of alpha alumina. Meyer (8) has reported that the temperature at which the transitional alumina transforms to alpha can be raised by incorporating a small amount of lithium oxide into the alumina powder that is used for spraying. This gives the coating an improved thermal stability. However, the most thermally stable coating of alumina, as well as the hardest, would be one that consisted entirely of the alpha phase. It is not impossible that some oxide or combination of oxides might be found that when added to the alumina powder before spraying, would catalyze the formation of alpha alumina when the particles are quenched. Although the refractoriness of the coating would undoubtedly be lowered by such an admixture, there are many applications for an alumina coating where a 2000°C melting temperature is not essential.

(3) Further investigation of stresses in the coating-metal system. Stresses in a coating oftentimes are a critical factor in determining whether or not the coating will perform satisfactorily for a given application. The stress work described in the present report is only a beginning. Obviously, a great deal of additional study will be necessary before these stresses can be completely understood.

(4) High-speed photography: A great amount of information about the forming of coatings by particle impact could be obtained by ultrahighspeed photography. The small size and high velocity of the particles present formidable difficulties. However, cameras with exposure times of as short as 0.1μsec. are now available and the use of such a camera together with suitable magnifying optics could prove highly rewarding.

ACKNOWLEDGEMENT

The authors are indebted to Bradley A. Peavy, Jr. of the Heat Transfer Laboratory at the National Bureau of Standards for performing the studies on heat transfer (Appendix II and III).

XV. REFERENCES

(1) Ault, Neil N., "Characteristics of Refractory Oxide Coatings Produced by Flame Spraying", J. Am. Ceram. Soc., 40, 69 (1957).

(2) Dickenson, Thos. A., "Flame Spray Ceramics", Products Finishing, Feb. 32 (1954).

(3) "Flame Plating Process", Steel, Aug. 30, 67 (1954). Also, Circular F-1184, "Flame Plating", Linde Co., 30 E. 42nd St., New York 17, N. Y. (1958).

(4) "Linde Starts Torch Service", Chem. & Eng. News, Dec. 15, 50 (1958).

(5) Ingham, H. S. and Shepard, A. P., Metallizing Handbook, Metco, Inc., 1101 Prospect Ave., Westburg, L. I., N. Y. (1959).

(6) Matting, A. and Becker, K., "An Experimental Investigation of the Metal Spraying Process", Electroplating and Metal Finishing, 8, 101-103, 143-145 (1955); also 9, 85-88, 126-128, 147-148 (1956). Also, Schweissen and Schneiden, 6, 127-142 (1954).

(7) Galli, J. R., Wheeler, G. I., Clampitt, B. H., German, D. E., and Johnson, R. B., "Development and Evaluation of Rocket Blast and Rain Erosion Resistant Composite Coatings Produced by Flame Spray Techniques", WADC Technical Report 58-493, Feb. 1959. Also, Astia Document No. 209913.

(8) Meyer, H. "Uber das Flammspritzen von Aluminiumoxyd", Werkstoffe and Korrosion, 11, 601-616, (Oct., 1960).

(9) Russell, A. S., Gitzen, W. H., Newsome, J. W., Ricker, R. W., Stowe, V. W., Stumpf, H. C., Wall, J. R., and Wallace, P., "Alumina Properties", Tech. Paper No. 10 (Revised), Aluminum Company of America, Pittsburgh, Pa. (1956).

(10) Roberts, A. G., "Improved Abrasive Jet Method for Measuring Abrasion Resistance of Coatings", Bull. Am. Soc. for Testing Mtls, No. 244, TP 52 (Feb., 1960).

(11) Moore, D. G., Hayes, W. D., Jr., and Crigler, A. W., "Velocity Measurements of Flame-Sprayed Aluminum Oxide Particles." WADC Technical Report 59-658 (October, 1959).

(12) Ingebo, Robert D., "Vaporization Rates and Drag Coefficients for Iso-octane Sprays in Turbulent Air Streams", NACA Tech. Note 3265 (Oct., 1954).

(13) Erwin, Guy, Jr., "Structural Interpretation of the Diaspore-Corundum and Boehmite - γ-Al_2O_3 Transitions", Acta Cryst. 5, 103 (1952).

(14) Plummer, M., "The Formation of Metastable Aluminas at High Temperatures", J. Appl. Chem. 8, 35 (1958).

(15) Foster, L. M., Long, G., and Hunter M. S., "Reactions Between Aluminum Oxide and Carbon. The Al_2O_3-Al_4C_3 Phase Diagram", J. Am. Ceram. Soc. 39, 1 (1956).

(16) Edgerton, H. E., "Flash, Seeing the Unseen by Ultra High-Speed Photography", p. 108, Charles T. Branford Co., Boston, Mass. (1954).

(17) Engel, Olive G., "Waterdrop Collisions with Solid Surfaces", J. Res. NBS, 54, 5, 281 (1955).

(18) Savic, P. and Boult, G. T., "The Fluid Flow Associated with the Impact of Liquid Drops on Solid Surfaces." Rept. MT-26, Natl. Res. Council of Canada, Ottawa, Canada (May, 1955).

(19) Brenner, Abner and Riddell, Grace, "Deposition of Nickel and Cobalt by Chemical Reduction", J. Res. NBS, 39, 385 (1947).

(20) Brown, S. D., "Room-Temperature Adhesive Tests of Various Flame-Sprayed and Flame-Plated Ceramic Coatings", Progress Rept. No. 20-374 from JPL to Ord. Corps, Dept. of Army (Jan. 8, 1959).

(21) Shepard, A. P., "Coating Evaluations", Special Company Report of Metco Inc., Westbury, Long Island, N. Y. (March, 1959).

(22) Heindlhofer, K., and Larsen, B. M., Trans. Am. Soc. of Steel Treating, 21, 865 (1933).

(23) Moore, D. G., Pitts, J. W., and Harrison, W.N., "Role of Nickel Dip in Enameling of Sheet Steel", J. Am. Ceram. Soc., 37, 363 (1954).

(24) Eubanks, A.G., Moore, D. G., and Pennington, W. A., "Effect of Surface Contour on the Oxidation Rate of Iron". (Paper has been prepared and will be submitted for publication in the Trans. of Am. Soc. for Metals.)

(25) Tylecote, R. F., "Factors Influencing the Adherence of Oxides on Metals", J. Iron and Steel Inst., 196, Pt. 2, 135-141 (Oct., 1960).

(26) Timoshenko, S., Analysis of Bi-Metal Thermostats, J. Opt. Soc. Amer., 11, 233-255 (1925).

(27) Engel, Olive G., "Pits in Metals Caused by Collision with Liquid Drops and Soft Metal Spheres", J. Res. NBS, 62, 6, 229 (1959).

APPENDIX I

PENETRATION OF HIGH-VELOCITY MOLTEN PARTICLES INTO METAL SURFACES

In a study of the particle-impact process it is important to know whether or not the molten particles penetrate the metal surface on impact. If such a penetration should occur, and if the coating material should form a continuous structure filling the cavities, then a mechanical interlock between the embedded particles and the metal might be expected. Such an interlock would be especially conducive to good bonding if significant undercutting occurred.

An analysis pertinent to this problem was completed recently by Dr. Olive Engle (27). The study was directed toward rain erosion, i. e., the damage caused on leading edges of high-speed aircraft and missiles when they pass through rain-filled clouds. A brief resume of her work is given below. This resume is followed by a description of several experiments designed to test the possible application of Dr. Engel's analysis to the microsized particles that must be dealt with in the spraying of particle-impact coatings.

First, consider a liquid drop colliding with a plane surface of a solid. At high speeds, the liquid drop acts in some respects as though it were a solid sphere, but unlike a sphere of hard solid material it undergoes an ultra-rapid radial flow. The degree to which the drop penetrates the surface of a solid metal, if it does penetrate, depends on (a) the density of the drop, (b) the collision velocity and (c) the dynamic strength properties of the solid surface. Liquid drops have less penetrating power than solid spheres do, because part of the collision energy is transformed into radial flow of the liquid.

Dr. Engel derived two generalized equations by use of dimensional analysis. The first gives the lowest drop velocity at which damage to the metal will occur. She terms this the intercept velocity, V_i.

$$V_i = \frac{19E'(z + z')}{(\rho c' z'^3)^{\frac{1}{2}}} \qquad (1)$$

where:

E' = dynamic compressive yield strength of metal.

z = acoustic impedance of drop liquid ($z = c\rho$ where c is velocity of sound through liquid and ρ is its density).

z' = acoustic impedance of metal

ρ = density of liquid

c' = velocity of sound through the metal.

Using this expression, V_i was computed for mercury drops of sizes ranging from 1.0 to 2.85 mm. diam. when impacting substrates of copper, iron, cold-rolled steel, lead and two aluminum alloys. The velocity of the mercury drop at which the first damage occurred is independent of drop diameter and varies from 7000 cm./sec. (197 ft./sec.) for lead to 37,000 cm./sec. (1214 ft./sec.) for cold-rolled steel. It is significant that experimental observations were in satisfactory agreement with computed values. Water droplets, which have lower density than mercury droplets, produced the first damage (the first penetration into the metal) at higher velocities than the drops of mercury. For example, for 2024-0 aluminum, the first damage occurred with mercury drops at 790 ft./sec.; with water droplets at 1540 ft./sec.

The second expression of interest relates the droplet diameter and velocity to the depth of the pit it forms.

$$\delta' = \frac{7.2\ d\ z}{c(z + z')} (V-V_i) \qquad (2)$$

where:

δ' = pit depth

d = diam. of droplet

V = velocity of droplet

V_i = intercept velocity

c = velocity of sound in liquid

This expression gives a straight line when V is plotted against δ'. The curves for mercury drops impacting copper are reproduced in Fig. 1A.

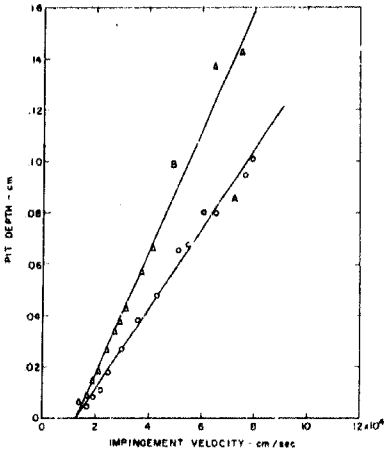

Figure 1A. Pit depths in copper caused by collisions with mercury droplets. Curve A is computed for 0.10-cm. drop and circled points are observed depths Curve B is calculated for 0.15-cm. drop and triangular points show observed values.

An attempt was made to apply Dr. Engel's expressions to alumina particles from the rod gun impacting polished surfaces of both sheet lead and sheet copper. In these calculations the density of the molten alumina was assumed to be 3.80 and the velocity of sound through the molten material was taken to be about the same as its velocity through water (1.50×10^5 cm./sec.). Using these assumed values in Equation (1), the particle velocity at which the first damage should appear on lead is 220 ft./sec. and on copper 614 ft./sec. The average velocity of alumina particles from the rod gun 6 in. from the nozzle is 444 ft./sec. Hence, if the assumed values for ρ and c for molten alumina are of approximately the right magnitude and if the minor amount of heating of the metal surface at the instant of impact did not change E' appreciably from its room-temperature value, then there should be penetration of the molten particles into polished lead at this distance but none into copper.

In testing this prediction, strips of lead 0.0148 in. thick and copper sheet 0.0168 in. thick were used. The specimens were sprayed with the rod gun at 6 in. from the nozzle. Numerous craters were observed in the polished lead. These ranged in depth from 1.0 to 4.0μ while the depth predicted by Equation (2) was 1μ for molten alumina droplets with a diameter of 25μ. Considering the assumptions that were made in the calculation, the observed penetration may be considered to be in fairly good agreement with Equation (2).

In a second test, a lead strip was sprayed with the rod gun at a distance of 12 in. from the nozzle. At this distance the particles have an average velocity of 350 ft./sec., which is still considerably above the calculated intercept velocity for lead (220 ft./sec.). Numerous pits were observed. Their depths were not measured but the penetrations were less than for the craters made at the 6 in. distance.

The computed intercept velocity for copper was 614 ft./sec., yet several tests showed that polished copper was damaged by particles having an average velocity of 444 ft./sec. The pits were too shallow for accurate measurement with the microscope but even the deepest were considerably under 1μ. Hence, for copper, damage occurs at a somewhat lower velocity than Equation (1) predicts. The poorer agreement for copper is not surprising. It could stem from such factors as damage to the copper by a few particles with velocities considerably above the average, as determined by the velocimeter, or localized heating of the copper that changed the room-temperature constants that were used in the calculations.

While the foregoing experiments give qualitative rather than quantitative confirmation of Equations (1) and (2), they nevertheless suggest that the relationships derived by Dr. Engel would be quantitatively applicable to flame-sprayed particles if the required parameters were known.

No solidified material was observed in any of the craters formed on the lead surface; hence, it is unlikely that bonding would be affected to an important degree by the shallow penetrations that occurred. However, at higher particle velocity there would be deeper penetration (see Equation (2)), and possibly if this penetration were sufficiently deep the particles would become imbedded in the metal, thus promoting a stronger bonding between the coating and the metal.

APPENDIX II.

DERIVATION OF EXPRESSIONS FOR SOLIDIFICATION RATES OF PARTICLES IN SPRAY

Assume that a molten sphere, initially at its freezing-point temperature throughout, is cooled at its outer surface by radiation and convection. The sphere will release its latent heat of fusion at the freezing temperature and solidification will occur at decreasing radii as a function of time. With the further assumption that the molten inner sphere does not develop a temperature gradient, the heat balance at the surface of the molten core may be expressed as follows:

$$-K\left(\frac{d\theta}{dr}\right)_{r=a} = L\,\rho\,\frac{da}{dt}$$

where:

θ = temperature difference between any stated point within the particle, and an arbitrary datum

r = radius in the solid shell

a = radius of molten core

L = latent heat of fusion

ρ = density of the freezing material

K = thermal conductivity of the solid

t = time

For the solid region from radius a, to the outside radius b, assume that the heat capacity changes are negligible, so that at all times the temperature, θ_r, at a radius, r, in the solid shell is substantially controlled by the radial heat flow:

$$\theta_r = \frac{a\theta_1[hb^2 - r(1-hb)]}{r[hb^2 + a(1-hb)]} \qquad (2)$$

where:

h = H/K

b = outside radius of sphere

H = $H_r + H_c$

H_r = coefficient of heat transfer (radiation)

H_c = coefficient of heat transfer (convection)

θ_1 = freezing temperature of molten material above ar arbitrary datum.

Differentiating (2) with respect to the radius, r, and substituting the value for r = a in (1) gives:

$$\frac{K\theta_1 hb^2}{a\,[hb^2 + a(1-hb)]} = L\rho \frac{da}{dt} \tag{3}$$

Integrating (3) with respect to time, t, and radius, a, using appropriate limits gives:

$$t = \frac{L\rho b}{6H\theta_1}\,[A + hbB] \tag{4}$$

where:

$A = 2[\,1-(a/b)^3\,]$

$B = 1 - 3(a/b)^2 + 2(a/b)^3$

Of particular interest is the ratio of the volume of the molten core to the volume of the sphere:

$$\text{Volume ratio} = \frac{4\pi(b^3-a^3)3}{4\pi b^3/3} \tag{5}$$

$$= \frac{A}{2}$$

If the value of hb in (4) is sufficiently small, the volume ratio is then a linear function of time.

The radiation component of the coefficient of heat transfer is obtained from the Stefan-Boltzman relation:

$$H_r = \frac{1.357\epsilon}{T_1 - T_2}\left[\left(\frac{T_1}{1000}\right)^4 - \left(\frac{T_2}{1000}\right)^4\right] \tag{6}$$

where:

H_r = radiation component

ϵ = emittance of sphere

T_1 = surface temperature of sphere

T_2 = temperature of surroundings

The determination of the convection component depends upon the temperature of the fluid (hot gases) surrounding the sphere. From McAdam's "Heat Transmission", Third Edition, p. 265, the convection coefficient is:

$$H'_c = 0.37\frac{k}{2b}\left(2b\rho V\right)^{0.6} \tag{7}$$

where:

k = thermal conductivity of fluid

ρ = density of fluid

V = velocity of fluid with respect to sphere

μ = viscosity of fluid

b = radius of sphere

The effective convection component becomes:

$$H_c = \frac{\theta_2 H_c'}{\theta_1} \qquad (8)$$

where θ_2 = temperature difference between surface of sphere and surrounding gases

$$\theta_1 = T_1 - T_2$$

APPENDIX III.

DEVELOPMENT OF EXPRESSIONS FOR HEAT TRANSFER OF SMALL MOLTEN MASSES OF MATERIAL IMPACTING SOLID SURFACES

Consider a substrate of thickness, a, with an instantaneous source of strength, Q, at x = a and time equals zero. For time greater than zero, heat is transferred from the two faces of the substrate by a combination of radiation and convection. Equation 4 of Carslaw and Jaeger (Heat Conduction in Solids, p. 298, Oxford Univ. Press, London, 1947) becomes for the surface of impact:

$$\theta_a = \frac{2Q}{a} \sum_{n=1}^{\infty} \frac{\beta_n^2 (\beta_n^2 + p^2) \exp\left[-\beta_n^2 \frac{\alpha t}{a^2}\right]}{\beta_n^4 + \beta_n^2 (p^2+s^2+p+s) + ps(ps+p+s)} \qquad (1)$$

where: θ_a = temperature rise above the initial temperature of the substrate

Q = strength of instantaneous source (defined later)

a = thickness of the substrate

$s = aH_1/K$

$p = aH_2/K$

K = thermal conductivity of substrate

H_1 = coefficient of heat transfer at x = 0

H_2 = coefficient of heat transfer at x = a

α = thermal diffusivity of substrate

and β_n are the positive roots of

$$\tan \beta = \frac{\beta(p+s)}{\beta^2 - ps}$$

Also, for the temperature at x = 0 (cold side)

$$\theta_o = \frac{2Q}{a} \sum_{n=1}^{\infty} \frac{(\beta_n^2+p)\ (\beta_n^2 \cos \beta_n + s\beta_n \sin \beta_n) \exp\left[-\beta_n^2 \frac{\alpha t}{a^2}\right]}{\beta^4 + \beta^2 (p^2+s^2+p+s) + ps(ps+p+s)} \qquad (2)$$

For computing the strength, Q, of the instantaneous heat source, all heat added above the initial temperature of the substrate must be included. Consider that a mass of sprayed material, M, per unit area is being sprayed onto a substrate. The initial temperature of the substrate is T_o. The sprayed material, which is at temperature, T, contains some latent heat of freezing, L, per mass

of sprayed material in a ratio, r, of mass of molten to total mass of material. The heat contained in the sprayed material is:

$$M\,[rL + C_s(T-T_o) + A + B]$$

where A and B are contributions due to impact of the sprayed material and impinging hot gases, respectively, and C_s is the specific heat of the sprayed material. This is equal to the product of strength and the volumetric heat capacity of the substrate, or:

$$Q = \frac{M}{\rho s}\,[rL + C_s(T-T_o) + A + B] \qquad (3)$$

For present purposes, the contribution due to energy release, A, at impact is considered negligible and while the contribution, B, due to heat from impinging hot gases is not negligible, its contribution is difficult to determine.

National Bureau of Standards, Washington, D. C
STUDIES OF THE PARTICLE-IMPACT PROCESS FOR APPLYING CERAMIC AND CERMET COATINGS, by D. G. Moore, A. G. Eubanks, H. R. Thornton, W. D. Hayes, jr., A. W. Crigler. August 1961. 52 p. incl illus. tables. (Project 8(88-7022); Task 70664) (ARL 59)

Unclassified Report

A basic study was made of the particle-impact process for applying coatings of aluminum oxide using both rod-type and power-type spray guns. High quenching rates - 800,000 C/sec. on stainless steel and 34,000 C/sec. on glass - induced the forma-

(over)

UNCLASSIFIED

tion of the softer eta phase of alumina. Size and velocity measurements were made for particles from both gun types. High speed motion pictures showed that powder guns sprayed particles continuously; the rod gun in bursts.

UNCLASSIFIED

UNCLASSIFIED

National Bureau of Standards, Washington, D. C
STUDIES OF THE PARTICLE-IMPACT PROCESS FOR APPLYING CERAMIC AND CERMET COATINGS, by D. G. Moore, A. G. Eubanks, H. R. Thornton, W. D. Hayes, jr., A. W. Crigler. August 1961. 52 p. incl illus. tables. (Project 8(88-7022); Task 70664) (ARL 59)

Unclassified Report

A basic study was made of the particle-impact process for applying coatings of aluminum oxide using both rod-type and power-type spray guns. High quenching rates - 800,000 C/sec. on stainless steel and 34,000 C/sec. on glass - induced the forma-

(over)

UNCLASSIFIED

tion of the softer eta phase of alumina. Size and velocity measurements were made for particles from both gun types. High speed motion pictures showed that powder guns sprayed particles continuously; the rod gun in bursts.

UNCLASSIFIED